

**NASA**  
**Technical**  
**Paper**  
**2992**

July 1990

# Diode Laser Satellite Systems for Beamed Power Transmission

M. D. Williams,  
J. H. Kwon,  
G. H. Walker,  
and D. H. Humes

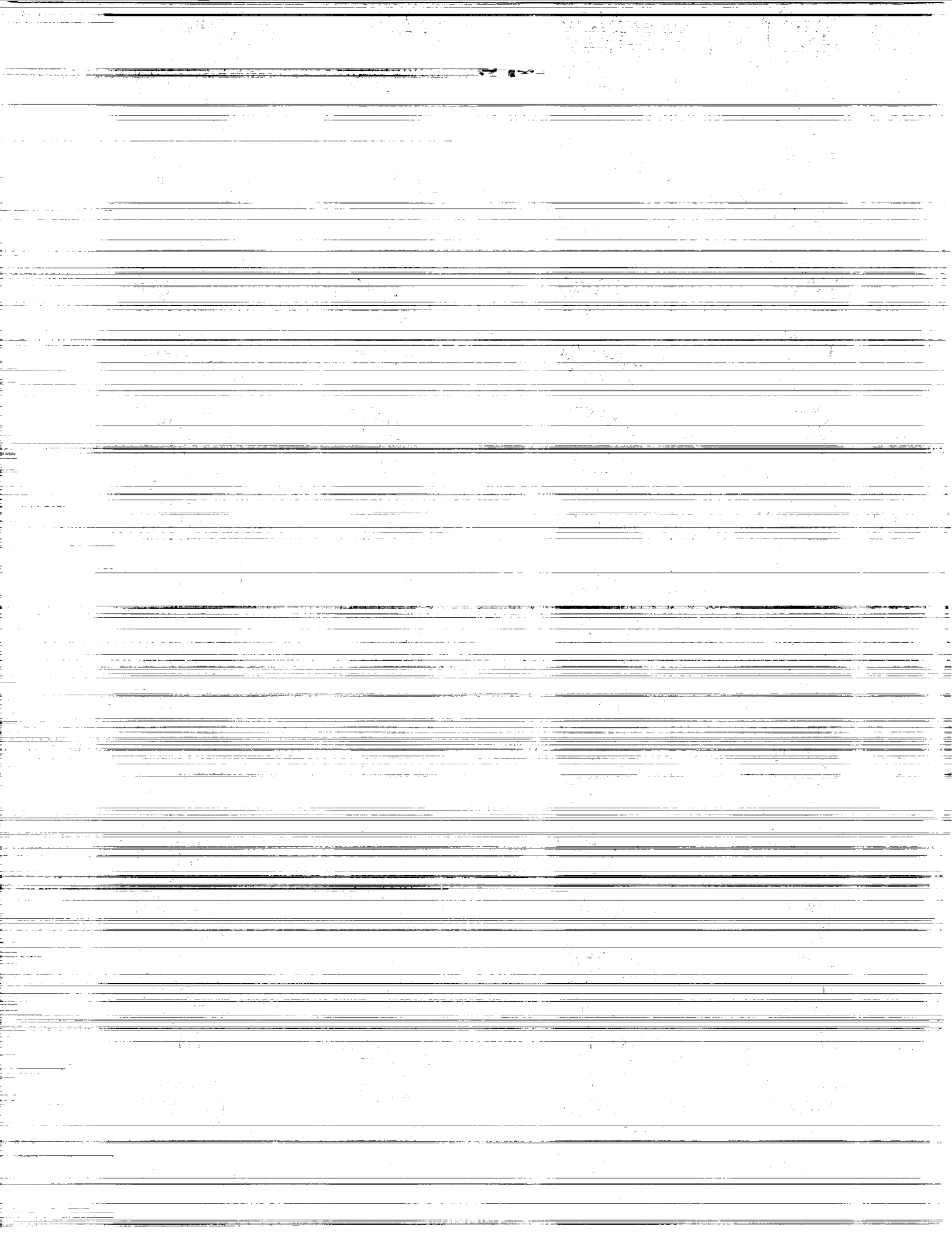
(NASA-TP-2992) DIODE LASER SATELLITE  
SYSTEMS FOR BEAMED POWER TRANSMISSION  
(NASA) 31 p

CSCL 20E

N90-24595

Unclass  
HI/36 0264756

**NASA**



**NASA  
Technical  
Paper  
2992**

1990

# Diode Laser Satellite Systems for Beamed Power Transmission

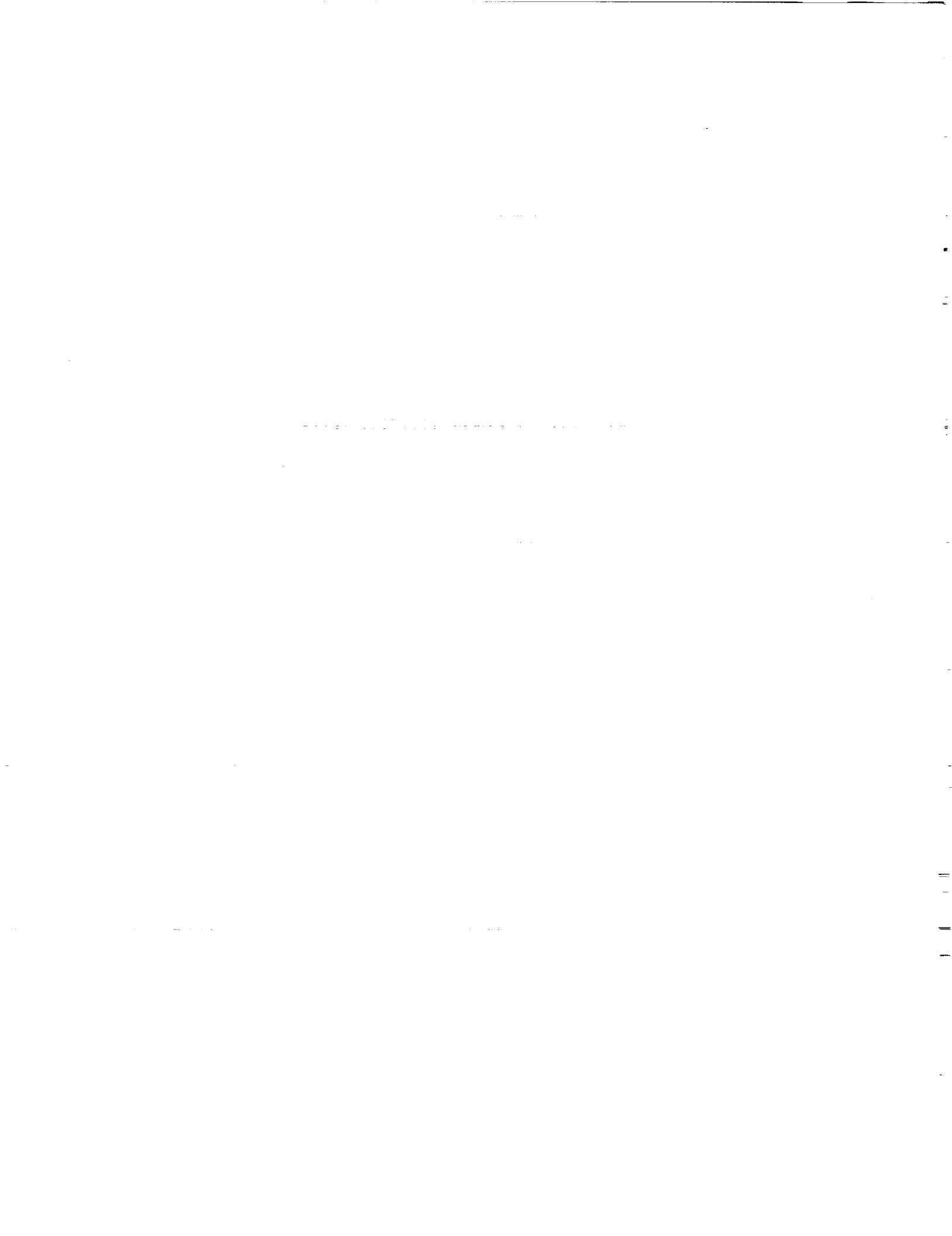
M. D. Williams  
*Langley Research Center  
Hampton, Virginia*

J. H. Kwon  
*Miami University  
Oxford, Ohio*

G. H. Walker  
and D. H. Humes  
*Langley Research Center  
Hampton, Virginia*

**NASA**

National Aeronautics and  
Space Administration  
Office of Management  
Scientific and Technical  
Information Division



## Summary

The concept of transmitting power in space by laser beam has received a major stimulus from the recent emergence and rapid advance of laser diode array technology. This technology, feasible projections of it, and other space systems technology are used to describe a generic system adaptable to many missions. Two specific and very different missions were chosen as a basis for a more detailed description.

The power system is composed of (1) a solar collector/concentrator, (2) a solar photovoltaic array, (3) a laser, (4) beam transmission optics, (5) heat radiators, and (6) a receiver/converter. These components are examined from a "systems" viewpoint. Sizes, masses, powers, etc., are provided for the two specific missions. Orbital information and critical technologies are also discussed.

This study shows a feasible and very promising implementation of space laser power transmission. The specific systems described are probably optimistic in that they postulate injection-locked laser amplifiers and large-scale, coherent beam combination, but expected advances in these technologies should make them realizable.

## Introduction

The idea of transmitting power from central power stations in space by using laser beams has been pursued by NASA since the early 1980's (refs. 1 and 2). The basic idea is to use a power source (e.g., nuclear or solar) to generate a powerful laser beam and transmit the beam, collimated and focused, to user locations where its power can be used as is or converted to other forms such as electrical or thermal power. Conceivably, one such system could serve the needs of many, as do central electric power stations on Earth. But more than that, such systems may provide the *best* means of accomplishing a scientific mission or offer capabilities not otherwise available. To assess these possibilities and to compare such systems with alternatives, one must describe the system, its requirements, and its capabilities. System description is the main objective here.

The availability of a number of power sources, lasers, power conversion schemes, and reception sites makes possible many implementations of a laser power transmission system. Each, theoretically, could be made to transmit a given amount of power, but each would differ in size, components, and/or transmission wavelength. The laser satellite described here (fig. 1) uses solar power, laser diodes, and photocells. (Satellites that use other lasers are described by recent studies in refs. 3, 4, and 5.) A

reception site and missions have been chosen to provide a framework for the description of two particular systems that differ greatly in power requirements and thus show the scalability and other attributes of the basic system. The two missions are (1) the provision of 1 MW of power to a lunar habitat similar to that described in reference 6 and (2) the provision of 75 kW to a large mobile lunar habitat/heavy-equipment rover (ref. 7). The satellites for both missions would circularly orbit the Moon 2000 km above its surface, a distance compatible with current pointing technology and the capability (if necessary) to provide continuous power transmission with three identical satellites to any point in view on the lunar surface. Inclinations of the orbits to the lunar pole assure almost continuous solar illumination of the satellites and produce an orbital precession that makes every point on the lunar surface accessible to power transmission at some time. The transmitting apertures of the satellites are large enough (8 m, or less, diameter) to provide beam spot sizes 1 m, or less, in diameter at the farthest transmission distance (lunar horizon). The apertures of parabolic reception dishes at user locations are large enough to encompass beam spots and the larger circular areas into which they will be transmitted due to pointing errors.

The transmission of power to the rover is believed to be a new and enabling technology. Powering the habitat by laser beam, though new, is not enabling and must be compared with other means of power provision. Regardless, such discussions are not within the main focus of this presentation, which is to describe a power transmission system that can be implemented many ways (possibly simultaneously), for many purposes, in many solar locations.

## Laser Satellite

### Solar Collector/Concentrator

The solar collector is integrated with heat radiators and together they form the largest, most massive structure of the satellite. It is a circular parabolic dish. The aperture of the collector must remain perpendicular to the Sun's rays and provide enough area to collect the power required by the satellite. The concave surface facing the sun is coated with silver and a protective layer of magnesium fluoride. The coatings reflect about 98 percent of visible radiation from the Sun. The outermost circular band of the collector does not incorporate heat radiators, except in a sector near the laser. (See fig. 1 and ref. 8. Fig. 1 shows this band and other bands for illustrative purposes only. They would not normally be visible in

the view shown.) The outer reflective band is assembled from smaller panels and has a mass density of  $0.1 \text{ kg/m}^2$ .

The wide middle band of the collector incorporates heat radiators on the dark side for cooling the solar photovoltaic array at the center of the collector. On the sunlit side, however, it forms a continuous reflective surface with the outer band. This reflective surface need not be "optical" quality because a precise image of the Sun at the array is not required.

Solar rays incident on the reflective surface of the collector are reflected toward the focus. (The outermost central ray would intercept the parabolic axis at a  $60^\circ$  angle.) Before arriving at the focal area, however, the rays are again reflected by a parabolic surface. This is a much smaller parabolic surface—the axis, focus, and convexity of which coincide with those of the collector. Its shape and position cause half of the incident radiant power to be reflected back toward the center of the collector in a quasi-collimated beam that is concentrated in power per unit area. Only that band of radiation (about 450 to 900 nm) that produces electricity in the photovoltaic array is reflected. Most of the radiation at other wavelengths is transmitted through the small parabolic dish and lost (but could be partially converted to electricity by several methods). To achieve this filtering action, the small parabolic dish must have a multilayer dielectric coating that faces the collector and a highly transmissive substrate.

### Solar Photovoltaic Array

The solar photovoltaic array is located at the center of the large parabolic reflector (collector). The array is composed of GaAlAs/GaAs cells and has a conversion efficiency of 22.5 percent at 353 K and a solar concentration of 300 (ref. 9). The diameter of the array is about the same as that of the small parabolic reflector. Light from the small parabolic reflector enters the array through a light diffuser designed to produce nearly uniform irradiance over the surface of the array. The heat sink of the array is thermally contacted to the radiator/collector structure described above. Electrical power from the array is transmitted through cables to the laser. The cables are routed through conduits down the back side of the collector.

### Laser

**Oscillator/Amplifier.** The smallest laser emitter is the "stripe," a single-quantum-well active region (typically  $0.1 \mu\text{m}$  thick  $\times 10 \mu\text{m}$  wide  $\times 200 \mu\text{m}$  long) inside a much larger GaAlAs/GaAs structure.

Single stripes can emit as much as 0.1 W of single-mode diffraction-limited power through the  $0.1 \mu\text{m} \times 10 \mu\text{m}$  face. A large number of stripes can be combined in a monolithic structure called a laser diode array (LDA) with the emitting faces lined up side by side in the same plane. (The linear dimension across all faces can approach 1 cm.) The stripes of an LDA are optically coupled to act as one powerful laser.

The advantages of LDA's are short wavelengths (0.7–0.9  $\mu\text{m}$ ), high electrical-to-optical conversion efficiencies (30–80 percent), compactness, long lifetime, high irradiance, and excellent beam quality (refs. 10–12).

Further, LDA's can be stacked so that the emitting faces line up in two directions. Feasibly, many LDA's can be combined in any two-dimensional pattern to form a large-scale array amplifier (LSAA) that can serve as a transmitting aperture. The transmitting aperture can approximate any shape and can have the dimensions of meters.

Beaming power to a spot in the far field requires the coherent combination and control of the emissions of many LDA's in an LSAA. The use of LDA's in injection-locking or amplification configurations can produce such nearly diffraction-limited beams (refs. 13–15). Several amplifier or injection-locked stages could be used for power scaling as shown in figure 2 (ref. 16). The number of LDA's in each stage is proportional to its input power so that each LDA receives the same power. If  $n$  stages each have gain  $G$  then

$$\left. \begin{aligned} P_0 &= P_1 G^n \\ n &= \log_{10}(P_0/P_1)/\log_{10} G \end{aligned} \right\} \quad (1)$$

where  $P_1$  and  $P_0$  are the output power of the master oscillator and the output power of the LSAA stage, respectively. For a gain of 100 per stage, 3 stages could produce a 1-MW output from a 1-W oscillator.

Since the LDA's are typically linear bars, as shown in figure 3, the input beam is focused into the LDA by a cylindrical lens, and the amplified output beam is collimated by a cylindrical lens. The output beam is Gaussian in the  $y$ -direction and nearly uniform in the  $x$ -direction.

**Far-field pattern.** Comparing the far-field patterns (FFP) of square and circular transmitting apertures of the same area and irradiance, there is more power in an Airy disk than in the central spot of a square aperture pattern. Hence, the overall shape of the large-scale output array is chosen to be circular.

The far-field diffraction pattern of a uniformly illuminated circular aperture is the Airy disk (ref. 17).

The main lobe of the pattern has a half-angle expressed by

$$\theta_1 \approx \frac{W}{Z} \approx \frac{1.22\lambda}{2w_o}$$

where

- $W$  beam radius at  $Z$  where amplitude decreases by a factor of  $e$
- $w_o$  beam radius at  $Z = 0$  where amplitude decreases by a factor of  $e$
- $Z$  transmission distance
- $\lambda$  transmission wavelength

Therefore

$$\begin{aligned} Ww_o &\approx 0.61\lambda Z \\ \pi^2 W^2 w_o^2 &= A_1 a_a \approx (0.61)^2 \pi^2 \lambda^2 Z^2 \\ A_1 a_a &\approx 3.67\lambda^2 Z^2 \end{aligned} \quad (2)$$

where  $A_1$  is the aperture area of the Airy disk and  $a_a$  is the aperture area of the transmitter.

The half-angle that includes the first ring is given by

$$\theta_2 \approx \frac{2.23\lambda}{2w_o}$$

The far-field amplitude produced at angles  $\alpha$  and  $\beta$  by a single element is

$$U_{ij}(\alpha, \beta) = C \int_{x_i^0 - D_x/2}^{x_i^0 + D_x/2} \int_{y_j^0 - D_y/2}^{y_j^0 + D_y/2} U_o(x, y) e^{ik(\alpha x + \beta y)} e^{i\phi_{ij}} dx dy \quad (5)$$

where  $(x_i^0, y_j^0)$  is the center coordinate of LDA amplifier element  $(i, j)$ ,  $\phi_{ij}$  is the phase error of the amplifier element with reference to the average phase of all LDA amplifiers,  $U_o(x, y)$  is the amplitude distribution at the output aperture of a single element,  $C$  is a constant, and  $k$  is  $2\pi/\lambda$ . The total amplitude is the summation over all LDA amplifiers:

$$U_t(\alpha, \beta) = \sum_i \sum_j U_{ij}(\alpha, \beta) = \sum_i \sum_j C \int_{x_i^0 - D_x/2}^{x_i^0 + D_x/2} \int_{y_j^0 - D_y/2}^{y_j^0 + D_y/2} F_{ij} U_o(x, y) e^{ik(\alpha x + \beta y)} e^{i\phi_{ij}^t(x, y)} e^{i\phi_{ij}^d} dx dy \quad (6)$$

where  $\phi_{ij}^t(x, y)$  and  $\phi_{ij}^d$  are the phase errors due to misorientation (tilt) and displacement of LDA amplifier element  $(i, j)$ , and  $F_{ij}$  is the failure factor

$$F_{ij} = \begin{cases} 0 & \text{(Failed)} \\ 1 & \text{(Good)} \end{cases} \quad (7)$$

The calculation was performed for two distributions of  $U_o(x, y)$ : (1) a one-dimensional Gaussian and (2) a two-dimensional Gaussian, that is,

$$U_o^I(x, y) = U_o \exp(-y^2/b^2) \quad (8)$$

Similarly,

$$A_2 a_a \approx 12.31\lambda^2 Z^2 \quad (3)$$

where  $A_2$  is the area enclosed by the outer circumference of the first ring.

However, the output array only approximates a uniformly illuminated circular aperture. The LDA elements are grouped inside the LSA as shown in figure 4. Each element produces a truncated two-dimensional Gaussian beam of rectangular symmetry (rather than a uniform beam). Each beam is collimated and coherent and each has dimensions of  $D_x$  and  $D_y$ . Only the detailed calculation that follows can give the true FFP and how various parameters affect it.

The full diffraction angles  $\theta_x$  and  $\theta_y$  of each beam are

$$\theta_x = \frac{2\lambda}{D_x} \text{ and } \theta_y = \frac{2\lambda}{D_y} \quad (4)$$

and are typically about 0.17 milliradian for  $\theta = 0.85 \mu\text{m}$  and  $D_x$  and  $D_y \approx 1 \text{ cm}$ .

Figure 5 illustrates the far-field geometry in one dimension. In two dimensions, the separation between the amplifiers is  $S_x$  and  $S_y$  along the  $x$ - and  $y$ -axes, respectively, and the fill factors are given by  $f_x = D_x/S_x$ ,  $f_y = D_y/S_y$ .

$$U_o^{II}(x, y) = U_o \exp\left(-\frac{x^2}{a^2} - \frac{y^2}{b^2}\right) \quad (9)$$

where  $a$  and  $b$  are constants. Therefore, the FFP's of the LSAA are given by

$$U_t^I(\alpha, \beta) = \sum_i \sum_j CU_o F_{ij} e^{i\phi_{ij}^d} \int_{x_i^0 - D_x/2}^{x_i^0 + D_x/2} \int_{y_j^0 - D_y/2}^{y_j^0 + D_y/2} e^{-(y^2/b^2)} e^{ik(\alpha x + \beta y)} e^{i\phi_{ij}^t(x, y)} dx dy \quad (10)$$

$$U_t^{II}(\alpha, \beta) = \sum_i \sum_j CU_o F_{ij} e^{i\phi_{ij}^d} \int_{x_i^0 - D_x/2}^{x_i^0 + D_x/2} \int_{y_j^0 - D_y/2}^{y_j^0 + D_y/2} e^{-(x^2/a^2 + y^2/b^2)} e^{ik(\alpha x + \beta y)} e^{i\phi_{ij}^t(x, y)} dx dy \quad (11)$$

Equations (10) and (11) have been programmed to produce the FFP of figure 6.

Figure 6 shows the central region of a typical FFP of the LSAA. Power collection efficiency 1 (PC1) is defined as the percent of total power inside the central spot (Airy disk); PC2 is the percent of total power in the central spot and its encircling ring. (The actual spot size of the Airy disk is 3 m for a 3087-km transmission distance and an LSAA diameter of 5 m. This spot wanders within another circular area determined by pointing accuracy.) The far-field beam pattern is affected by the number of LDA amplifiers, tilt and displacement phase errors, and random failures of the LDA amplifiers. Since the FFP is determined by integration of phase and amplitude distribution over the LSAA aperture, PC1 and PC2 are almost independent of the number of LDA amplifiers. High-order diffraction losses cause PC1 and PC2 of the LSAA to be smaller than the corresponding efficiencies of a simple circular aperture.

When there are tilts of wave fronts among LDA amplifiers, the power collection efficiencies are affected. For the one-dimensional analysis, preliminary calculations show that tilts as large as 25 percent of the amplifier diffraction angle (eq. (2)) have little effect on PC1 and PC2. Because tilt phase errors are cancelled out when integrating across the aperture in the far field, their only effect is a shift in position of peak intensity without any phase change. Therefore, the required parallelism among the output beams of the LDA amplifiers is less than 25 percent of the amplifier diffraction angle. Displacement phase errors have a large influence on the FFP, PC1, and PC2 because these phase errors are cumulative when integrating over the LSAA. The displacement phase error of amplifier ( $i, j$ ) is

$$\phi_{ij}^d = k \Delta d_{ij} \quad (12)$$

where  $\Delta d_{ij}$  is the displacement of the wave front ( $i, j$ ) from the reference wave front. Random numbers

generate displacement phase errors for all LDA's within a limit value. (Each error within the limit is equally probable.) Figure 7 shows the decrease of the power collection efficiencies PC1 and PC2 as a function of the limit of displacement phase error. Efficiencies PC1 and PC2 decrease significantly when the displacement phase error limit is increased from 0 to  $0.5\lambda$ . The solid and dashed curves represent one-dimensional (eq. (8)) and two-dimensional Gaussian profiles (eq. (9)), respectively. They show almost the same effects except for a small difference in the power collection efficiencies. When random failures of LDA amplifiers are allowed, the effect is almost the same except for a few percent decrease in the power collection efficiencies.

The maximum allowable limit of displacement phase error is about  $0.15\lambda$  for an 80-percent power collection efficiency (PC2). If phase matching among the element amplifiers can be done within  $0.1\lambda$ , then PC1 is 78 percent and PC2 is 88 percent. Power reception efficiency is also dependent on the receiver aperture size and transmitter pointing accuracy. A value of 85 percent is used for system calculations.

The finite probabilities of failures of individual LDA's cause a variation in power reception efficiency. Power reception efficiency decreases about 4 percent if 40 percent of the LDA's fail. This decrease is small because the central part of the FFP is relatively unaffected by failures of LDA amplifiers, but power in the entire FFP decreases proportionately.

## Beam Transmission Optics

Beam transmission optics consist of a fixed gas lens and a low-mass flat director mirror. The beam from the laser output array is collimated (flat wave front) and intercepts the gas lens first. The gas lens induces an extremely small radius of curvature in the wave front, and the beam proceeds to the director mirror, where it is reflected toward the receiver location.

**Gas lens.** The gas lens illustrated in figure 8 is a transparent vessel containing gas at a variable pressure. It would probably best be implemented as a plano-convex vessel containing helium. The plano-convex configuration would provide ease of construction and nearly minimum aberration. The entrance and exit surfaces are coated with thin films to optimize transmission and compensate for the small radial phase differences caused by the curvature of the uniformly thick material. Neither the coating, the vessel material, nor the gas absorb radiation at the laser wavelength. Essentially all the wave front curvature is caused by the gas inside the vessel. Varying the gas pressure varies the amount of induced curvature and the effective focal length of the lens. For example, a lens with a 10-m convex radius of curvature would focus laser radiation at 3310 km for a pressure of approximately 1.9 mm of mercury. (The distance to the horizon from 2000 km above the Moon's surface is 3310 km.)

**Director mirror.** The director mirror rotates about two axes: one perpendicular to the orbital plane of the satellite, the other perpendicular to the first. Rotation about each axis must provide horizon-to-horizon coverage of the surface below. The director mirror is circular. Its diameter is large enough to intercept the entire laser beam at the beam's greatest angle of incidence. It must also be strong, lightweight, and flat within a fraction of the laser wavelength.

An alternate method for pointing the laser beam would be to electronically control the phases of the light waves from the diodes. Use of this method might eliminate the need for a gas lens and director mirror, substantially reduce the mass of the satellite, and provide almost instantaneous pointing response. Indications are, however, that such a system would be unable to provide the required range of pointing angles while providing receiver spot sizes smaller than the transmitter dish. That technology might provide the small angular changes needed by a servo feedback loop to improve tracking accuracy and reduce the size of the reception dish.

## Satellite Radiators

**Main radiator.** The main radiator radiates waste heat from the photovoltaic array into space. Physically, it is an aluminum sheet that uses heat pipes to distribute heat uniformly and provide additional structural stiffness. The Sun side of the radiator provides a substrate for the reflective coatings. As described in reference 18, its mass density

is  $2.5 \text{ kg/m}^2$ . Its surface, being approximately perpendicular to any surface that it orbits, absorbs very little radiation from that surface. Neither does it absorb radiation directly from the Sun (it is shaded) or from itself (on its convex side). (Its concave side reabsorbs a small part of its own radiation.) The orientation and shape of the main radiator make it an effective radiator even at relatively low temperatures.

**Laser radiator.** Radiation of waste heat from the laser is accomplished by a separate radiator operating at a lower temperature and located closer to the laser. The housing and support structure of the laser form part of the radiator. The main part of the laser radiator, however, is located in a band sector centered on the bottom (nadir) side of the collector. In this position it "sees" little radiation from the main radiator. The laser, laser radiator, and transmission optics, all being located on the lower (nadir) side of the otherwise symmetrical satellite system, provide gravity gradient stabilization of the satellite and reduce the amount of thrusting needed for its reorientation during orbit.

## Laser Converter Assembly

### General

The laser beam from the satellite is directed to the laser converter assembly to convert the laser photons to electricity. The output of the converter assembly is used to power a fixed lunar base or to power a lunar rover that can cover nearly 100 percent of the lunar surface. The electrical output power is 1 MW for the habitat and 75 kW for the rover. Figure 9 is a flow diagram for the laser converter assembly. The laser beam is incident on a highly reflective parabolic dish that redirects the beam toward the photovoltaic converter from wherever pointing accuracy may have placed it. The reception dish also acts as a secondary concentrator that adjusts the beam size to that of the photovoltaic converter. A lenticular array of small antireflection-coated lenses in front of the converter evenly distributes the laser beam intensity over the area of the photovoltaic converter where the laser photons are converted to electricity. The electrical power then passes through the appropriate power-conditioning equipment to the user (either the habitat or the rover). Although the photovoltaic converter has a high efficiency, a significant amount of heat must be removed. In order to accomplish this, the photovoltaic converter is mounted on a heat pipe that transfers the heat to a radiator. Each component of the laser converter assembly will be discussed in more detail.

## Photovoltaic Converters

Photovoltaic converters have been used for many years to convert solar radiation to electricity; however, conversion of laser photons to electricity requires some additional considerations. Laser radiation is monochromatic, whereas solar radiation is broadband. Laser irradiance is high (up to  $1 \text{ kW/cm}^2$ ), whereas the irradiance for unconcentrated solar radiation is low ( $\approx 0.136 \text{ W/cm}^2$ ).

In order to maximize the laser-to-electric conversion efficiency, the bandgap energy of the converter semiconductor must be very near the laser photon energy (ref. 19). The wavelength of the diode laser used in this laser-power system is  $0.85 \mu\text{m}$ . This wavelength requires a semiconductor bandgap energy of  $1.46 \text{ eV}$  in order to maximize the converter efficiency. Although there is no binary semiconductor with this bandgap energy, the composition of the ternary semiconductor  $\text{Ga}_{1-x}\text{Al}_x\text{As}$  can be adjusted to achieve this bandgap ( $x$  is the fraction of Al). The relationship between the bandgap energy and the composition is  $E_g = 1.424 + 1.247x$  (ref. 20) where  $E_g$  is the bandgap energy in electron volts and  $x$  is the fraction of Al. The compound  $\text{Ga}_{0.971}\text{Al}_{0.029}\text{As}$  has a bandgap energy of  $1.46 \text{ eV}$  at  $300 \text{ K}$ . This semiconductor would be appropriate for use with a  $0.85\text{-}\mu\text{m}$  diode laser.

Figure 10(a) is a diagram of a conventional photovoltaic converter (not to scale). In a conventional converter, the photons are incident normal to the  $p$ - $n$  junction. The charge carriers, after being separated at the  $p$ - $n$  junction, must then diffuse laterally and vertically to reach the metal contacts.

Figure 10(b) is a diagram of a *vertical* junction converter (not to scale). In this type of device, the photons are incident parallel to the  $p$ - $n$  junction. Each face of the converter is completely covered with the contact metal. The charge carriers can thus diffuse a short distance to the metal contacts without having to diffuse laterally through the higher resistivity semiconductor material. This property minimizes the series resistance of the converter, an important consideration in efficient conversion of high-intensity laser radiation to electricity. For this reason, the vertical junction photovoltaic converter was selected as the laser converter.

In order to obtain the highest practical laser-to-electric conversion efficiency, the vertical junction converter was optimized using the model described in reference 21. Table I lists the optimized converter parameters for use with a  $0.85\text{-}\mu\text{m}$  diode laser. These parameters were optimized for a single vertical junction converter. However, a practical converter would consist of many single junctions con-

nected in series. Figure 11 shows the efficiency of a 500-junction, series-connected converter as a function of input power density. The efficiency increases from 26 percent at  $1 \text{ W/cm}^2$  to 47 percent at  $1 \text{ kW/cm}^2$ . A power density of  $1 \text{ kW/cm}^2$  is chosen for the habitat and  $0.1 \text{ kW/cm}^2$  is chosen for the rover. The converter efficiency is 47 percent for the habitat and 32 percent for the rover.

## Converter Radiators

Although these efficiencies are quite high, a substantial amount of the incident photons are converted to heat that must be removed to keep the converter temperature at  $300 \text{ K}$ . In this space power system, the most convenient method of heat removal is by radiation to space using heat pipe radiators (ref. 18). In order to electrically insulate the converter vertical junctions from the heat pipe, the converter is mounted on a diamond sheet. This diamond sheet provides good electrical insulation and also high thermal conduction (ref. 22) for conducting the heat away from the converter. Figure 12 is a schematic diagram of this type of converter system. The lunar base radiator is mounted on an insulating blanket to prevent heat transfer from the surface and is aligned with the solar ecliptic to prevent direct solar irradiation. The area needed for the respective radiators was calculated from

$$A = \frac{q}{\sigma\epsilon(T_1^4 - T_2^4)} \quad (13)$$

where

$q$  heat radiated,  $1.1 \text{ MW}$  (for lunar habitat) and  $0.16 \text{ MW}$  (for lunar rover)

$A$  radiator area

$\epsilon$  emissivity, 1

$\sigma$  Stefan Boltzmann constant,  $5.7 \times 10^{-8} \text{ W}\cdot\text{m}^{-2}\cdot\text{K}^{-4}$

$T_1$  temperature of radiator,  $300 \text{ K}$

$T_2$  temperature of heat sink,  $250 \text{ K}$  (ref. 23)

The radiator area needed for the lunar habitat is  $4.6 \times 10^3 \text{ m}^2$  and for the rover is  $6.7 \times 10^2 \text{ m}^2$ . From reference 18, the specific mass of a typical radiator is  $4 \text{ kg/m}^2$  (for a radiator that radiates from one side only). Here, the same radiator radiates from two sides. Therefore, its specific mass is  $2 \text{ kg/m}^2$ . The mass of the habitat radiator is  $9.2 \times 10^3 \text{ kg}$ , or 98.6 percent of the total habitat converter system mass. The mass of the rover radiator is  $1.3 \times 10^3 \text{ kg}$  or 97.0 percent of the total rover converter system mass.

### **GaAlAs, Diamond Substrate, and Lenticular Diffuser**

The area of GaAlAs needed for the converter was calculated from the required efficiency, input power density, and output power. Using the thickness and density, the mass of GaAlAs is calculated to be 0.01 kg for the habitat and 0.01 kg for the rover. The 1-mm-thick diamond substrate has the same area as that of the GaAlAs. The mass of the diamond substrate is 0.4 kg for the lunar habitat and 0.8 kg for the rover. The 1-mm-thick lenticular diffuser has the same area as the GaAlAs. The mass of the lenticular diffuser is 0.6 kg.

### **Supporting Structure, Supporting Blanket, Secondary Concentrator, and Insulating Blanket**

The supporting blanket is typical of that used with solar arrays. Using a specific mass of  $2.7 \text{ kg/m}^2$ , the mass of the supporting blanket is 2.7 kg for the lunar habitat and 0.7 kg for the rover. The aluminum support structure consists of an aluminum plate and four aluminum support rods. The mass of this supporting structure is 116 kg for the lunar habitat and 31.8 kg for the rover. The polished secondary concentrator focuses the larger laser beam down to the diameter of the converter. The mass of the secondary concentrator is 6.7 kg for the lunar habitat and 7.0 kg for the rover. Table II shows the masses of the converter system components for both the 1-MW habitat and the 75-kW rover.

### **Component Parameters**

Component parameters are calculated by working backward from the mission power requirement. The rover on the lunar surface requires 75 kW of power. Analysis of the laser photoconverter shows that it can convert 32 percent of the laser power that it receives to electrical power. (The other 68 percent must be radiated away as waste heat.) Therefore, it must receive 234 kW. The photoconverter receives only 85 percent of the transmitted radiation because the diffracted beam is larger than the area of the photoconverter, so about 276 kW must be transmitted by the laser optics. (Refer to figs. 13 and 14.) Since there is negligible attenuation in the transmission optics, the power from the laser must also be 276 kW. (Various parameters, some of which are presented here parenthetically for convenience, are summarized in tables III and IV.)

The laser amplifier is composed of three injection-locked stages, the output array being the final stage. Each stage amplifies power by a factor of 100 by increasing the number of LDA's while maintaining the

power of each at 5 W. The LDA's in the output array (55 148) produce an output power that is the nearest multiple of 5 W greater than the power required by the receiver/converter. Adding the LDA's of the other two stages and a driver, the total number of LDA's in the laser is 55 705. Input power to the amplifier must be supplied to all these LDA's (not just the output stage). That requires an input power of 0.398 MW, since the LDA's operate at 70 percent efficiency in the injection-locked mode. Input power in excess of output power must be radiated to space.

The solar photovoltaic array at the center of the parabolic dish must provide the input power to the laser amplifier. The photovoltaic array operates at 22.5 percent efficiency when illuminated by power from the whole solar spectrum. The whole solar spectrum does not illuminate the array, but the array operates as if it were illuminated by all the solar spectral power reflected from the parabolic collector. So the collector must reflect 1.77 MW, and its aperture must collect 1.8 MW. (The collector absorbs 36.1 kW.) In the vicinity of the Earth and the Moon, the Sun provides an irradiance of  $1365 \text{ W/m}^2$ . The small parabolic reflector near the focus of the collector spectrally divides the 1.77 MW from the collector. Only the effective half (as explained above) reaches the photovoltaic array. The difference between the effective half (0.88 MW) and the array output power (0.398 MW) must be radiated away as heat.

The photovoltaic array functions optimally near a solar concentration of 300, so its area is the collector aperture area multiplied by the reflectivity (0.98) and divided by 300. The diameters of the photovoltaic array and the small parabolic reflector are equal. The focal length of the collector is 17.8 m, and its diameter is 41 m.

The main radiator and laser radiator areas are determined by equation (13) with the exception that the emissivities of the areas are 0.95 and 0.5 for the back side and front side of the collector, respectively. Radiation areas of the laser housing and its supports have not been included.

(Analysis of the habitat system follows the same above procedure.)

The gas lens and director mirror are the major components of the transmission optics in terms of function and mass. The area of the lens approximates that of the laser beam. For the habitat beam, the mass, based on 5.0-mm-thick silicate glass, is about 1075 kg. Including structure, the total mass of the lens system is 1255 kg.

The mirror diameter must be twice the diameter of the laser beam to be able to redirect the entire beam to all the visible surface below. Although its surface area is four times that of the lens, its mass

can be kept relatively small by use of the graphite epoxy and honeycomb technology associated with the Advanced Sunflower mirrors. Its mass (habitat beam) is estimated at 800 kg. The slewing and acceleration required of the mirror is very small and can be provided by two small electric motors with appropriate gearing. The masses of the motors and gears are expected to be about 90 kg. The total mass of the mirror system is estimated to be 1020 kg. Corresponding masses for the rover beam optics are given in table III.

Transporting the laser power station from low Earth orbit (LEO) to lunar orbit requires the additional masses of an orbit transfer vehicle (OTV) and the fuel required for its operation. Transporting the receiver/converter from LEO to lunar orbit and then to the lunar surface requires an OTV, its fuel, and a lunar descent vehicle and its fuel. (These masses are included in tables II, III, and IV to facilitate comparisons with other sources of power for use on the lunar surface and for the lunar rover.) Estimates of these transportation masses are based on the performance of the chemical propulsion OTV's discussed in references 24 and 25. They include all the fuel required to deliver the cargo to or near the Moon and to return the unloaded OTV to LEO. They also include an appropriate fraction of the OTV mass because, while the OTV's are reusable, they have a projected lifetime of about 30 missions.

The mass needed to transport cargo to or near the Moon greatly exceeds the mass of the cargo itself. (Fig. 15 graphically portrays the relative sizes of component masses and their totals.) Delivery to lunar orbit was found to require a transportation mass that was 1.7 to 2.2 times the cargo mass, depending on the size of the OTV. Large OTV's were more efficient. Delivery to the lunar surface was found to require a transportation mass that was 4.15 times the cargo mass when the cargo mass was about 20 000 kg. The data in reference 25 limited the calculation to this single value, which was applied to the delivery of cargo of any size to the lunar surface.

The mass of fuel required to orient the satellite would depend strongly on its lunar precession (which has not been calculated) and has not been included in the mass estimates. The use of high-specific-impulse ion thrusters is expected to limit that required mass to a very small amount.

### Orbit and Power Distribution

Orbits affect the shape, size, duty cycle, coverage, and orientation of the transmitter/converter system and, in turn, are determined primarily by system pointing accuracy, allowable transmitter/converter sizes, and transmission wavelength. For example, a

satellite beam to the lunar horizon (3310 km) would require a receiving (converter) dish at least 6.62 m in diameter if pointing accuracy is 1 microradian. (Ref. 26 indicates that 1 microradian is achievable.) Any finite spot size would increase the required diameter. Spot area, transmission distance, and beam wavelength are related to the area of a uniformly radiating transmitter aperture by equation (2).

Transmission distance is determined by orbit height and the position of the converter on the surface. Orbit height and geometry determine the instantaneous velocity of the satellite. For a circular lunar orbit, velocity is constant and is given by

$$V = [GM/(R + h)]^{1/2} \quad (14)$$

where

- $G$  universal gravitational constant
- $M$  mass of the Moon
- $R$  radius of the Moon
- $h$  orbit altitude

The period of the orbit and surface areas covered (fig. 16) can be calculated from the velocity and altitude.

Lunar orbit was chosen to be circular at an altitude of 2000 km. At that altitude, the best practical pointing accuracy (approximately 1 microradian) requires a receiver dish several meters in diameter for expected transmitter apertures. The orbit must pass within  $50^{\circ}29'$  of the lunar pole to receive constant solar illumination. A much closer approach to the lunar pole would provide a more favorable alignment of satellite components for gravity gradient stabilization, but the actual inclination of orbit would be chosen to minimize the thrust needed to keep the collector facing the Sun as the satellite precesses about the Moon. Precession of the satellite would provide complete coverage of the lunar surface over a period of time.

Three satellites approximately  $120^{\circ}$  apart in orbit would be required to provide uninterrupted power to a single user within 654 km of the orbital plane on the lunar surface. (Orbital precession would eventually interrupt power flow to a stationary receiver.) Receivers more than 654 km from the orbital plane would not be powered constantly; the farther from the orbital plane, the smaller the duration of power reception. Power would be received on the surface as far away as 1889 km from the orbital plane. Multiple users with power links would extend the duration of power reception and/or decrease the number of satellites required. In an extreme example, three

linked receivers 120° apart on the surface could receive constant power from one satellite. That one satellite would have to be three times more powerful to maintain the power levels at each station. (But the power levels need not necessarily be maintained. Up to three times as much power would be available on demand at any particular site.) A satellite power system might "bootstrap" such power links on the lunar surface by use of the rover.

## Critical Technologies

### Laser Diodes

In the satellite system described here, the LDA's operate at 70 percent efficiency. This efficiency has been obtained (ref. 27) at an operating temperature of 300 K but approaches an upper limit of present capability. Efficiencies as large as 84 percent are possible (ref. 28). However, LDA's of these high efficiencies are not yet mass produced. Also, if such high efficiencies are obtained at high operating current densities, the lifetime of the LDA is adversely affected (ref. 29). Currently, LDA's operating at about 1000 A/cm<sup>2</sup> and 300 K can operate constantly for approximately 1 year with continuous degradation. Elevated operating temperatures significantly degrade efficiency and lifetime and affect output wavelength (refs. 30 and 31). The extreme heat flux densities generated by LDA's make heat transfer design very sensitive.

### Beam Combination

A number of methods exist for combining laser beams coherently (refs. 16 and 32). Among these are the traveling-wave amplifier and the injection-locked amplifier. The system described here assumes that an injection-locked amplifier is used. With injection locking, individual elements of the output array can operate at their oscillator power level (5 W) while combining coherently (ref. 17). However, injection locking is very sensitive to temperature changes and is very difficult to implement. The use of a traveling-wave amplifier, on the other hand, would produce less power per LDA but would be easier to implement. If injection-locked amplifiers prove to be impractical, the expected development of larger and/or two-dimensional LDA's could more than compensate for the loss of power per LDA.

The critical technologies impact two important parameters of the satellite system: laser diode efficiency and laser beam coupling efficiency. Figures 17 and 18 show their effects on total satellite mass. Laser diode efficiency will depend on the development of laser diode technology and how

laser diodes are implemented in amplifiers. Beam coupling efficiency can be altered by (1) the distance between transmitter and receiver, (2) the sizes of transmitter and receiver, (3) laser beam coherence, (4) pointing/tracking errors, and (5) optical accuracies.

### Photovoltaic Converter

The particular configuration of the Ga<sub>0.971</sub>Al<sub>0.029</sub>As vertical junction converter has never been fabricated. Molecular beam epitaxy or vapor phase epitaxy can be used to grow structures of the required dimensions. Interconnection of the *p-n* junction units requires a metal that will grow as a single crystal on Ga<sub>0.971</sub>Al<sub>0.029</sub>As. This technology has not been demonstrated and is critical to the fabrication of the converter.

### Concluding Remarks

The satellite system described here does not include (1) the very highest laser diode array (LDA) power efficiency that is possible, (2) the highest power per LDA that is available today, (3) the best reception efficiency that could be achieved, or (4) the maximum use of available solar power. It has included (1) a high large-scale array amplifier efficiency, (2) injection-locked amplifiers, (3) coherent beam combination, and (4) advanced lithographic technology for diode lasers. The extremely rapid development of these technologies should make them a reality within a decade and justifies their inclusion.

Though this description applies to lunar missions, such satellites can be used at other locations in the solar system for other missions. For example, they could provide power at the asteroid belt, which is expected to be a source of raw materials for future space development. For Earth itself, they offer pollution-free power for the projected demands of emerging nations in the next several decades.

Power sources other than the Sun could drive the laser transmitter. Only one, the nuclear reactor, is competitive. Although nuclear power is a viable option, its development and use is more a political issue than a scientific or utilitarian issue.

That a similar satellite system could be made today testifies to its imminence. The degree of perfection to which the critical technologies can develop (and how soon they develop) will determine how well (and how soon) these satellites compare with the description given here.

NASA Langley Research Center  
Hampton, VA 23665-5225  
April 26, 1990

## References

1. Wilson, J. W.; and Lee, J. H.: Modeling of a Solar-Pumped Iodine Laser. *Virginia J. Sci.*, vol. 31, no. 3, Fall 1980, pp. 34-38.
2. Williams, M. D.; and Conway, E. J., eds.: *Space Laser Power Transmission System Studies*. NASA CP-2214, 1982.
3. De Young, R. J.; Walker, G. H.; Williams, M. D.; Schuster, G. L.; and Conway, E. J.: *Preliminary Design and Cost of a 1-Megawatt Solar-Pumped Iodide Laser Space-to-Space Transmission Station*. NASA TM-4002, 1987.
4. De Young, R. J.; Lee, J. H.; Williams, M. D.; Schuster, G.; and Conway, E. J.: *Comparison of Electrically Driven Lasers for Space Power Transmission*. NASA TM-4045, 1988.
5. De Young, Russell J., ed.: *Second Beamed Space-Power Workshop*. NASA CP-3037, 1989.
6. Mason, Lee S.; and Bloomfield, Harvey S.: SP-100 Power System Conceptual Design for Lunar Base Applications. *Transactions of the Sixth Symposium on Space Nuclear Power Systems*, Mohamed S. El-Genk and Mark D. Hoover, eds., Inst. for Space Nuclear Power Studies, 1989, pp. 9-12.
7. Friedlander, Alan; and Cole, Kevin: Power Requirements for Lunar Base Scenarios. Symposium on Lunar Bases and Space Activities in the 21st Century, LPI Contribution No. 652, Lunar and Planetary Inst., 1988, p. 85.
8. Canady, John E., Jr.; and Allen, John L., Jr.: *Illumination From Space With Orbiting Solar-Reflector Spacecraft*. NASA TP-2065, 1982.
9. Hamaker, H. C.; Grounner, M.; Kaminar, N. R.; Kuryla, M. S.; Ladle, M. J.; Liu, D. D.; MacMillan, H. F.; Partain, L. D.; Virshup, G. F.; Werthen, J. G.; and Gee, J. M.: 25%-Efficient GaAs Cassegrainian Concentrator Cell. *Space Photovoltaic Research and Technology 1988—High Efficiency, Space Environment, and Array Technology*, NASA CP-3030, 1989, pp. 292-297.
10. Botez, Dan; and Ackley, Donald E.: Phase-Locked Arrays of Semiconductor Diode Lasers. *IEEE Circuits & Devices Mag.*, vol. 2, no. 1, Jan. 1986, pp. 8-17.
11. Botez, D.; Mawst, L.; Hayashida, P.; Peterson, G.; and Roth, T. J.: High-Power, Diffraction-Limited-Beam Operation From Phase-Locked Diode-Laser Arrays of Closely Spaced "Leaky" Waveguides (Antiguides). *Appl. Phys. Lett.*, vol. 53, no. 6, Aug. 8, 1988, pp. 464-466.
12. Cross, Peter S.; Harnagel, Gary L.; Streifer, William; Scifres, Donald R.; and Welch, David F.: Ultrahigh-Power Semiconductor Diode Laser Arrays. *Science*, vol. 237, no. 4820, Sept. 11, 1987, pp. 1305-1309.
13. Abbas, Gregory L.; Yang, S.; Chan, Vincent W. S.; and Fujimoto, James G.: Injection Behavior and Modeling of 100 mW Broad Area Diode Lasers. *IEEE J. Quantum Electron.*, vol. 24, no. 4, Apr. 1988, pp. 609-617.
14. Andrews, John R.: Traveling-Wave Amplifier Made From a Laser Diode Array. *Appl. Phys. Lett.*, vol. 48, no. 20, May 19, 1986, pp. 1331-1333.
15. Goldberg, L.; Taylor, H. F.; Weller, J. F.; and Scifres, D. R.: Injection-Locking of Coupled Stripe Diode Laser Arrays. *Appl. Phys. Lett.*, vol. 46, no. 3, Feb. 1, 1985, pp. 236-238.
16. Kwon, J. H.; Williams, M. D.; and Lee, J. H.: *A Survey of Beam-Combining Technologies for Laser Space Power Transmission*. NASA TM-101529, 1988.
17. Siegman, Anthony E.: *Lasers*. Univ. Science Books, c.1986.
18. French, Edward P.: Heat-Rejection Design for Large Concentrating Solar Arrays. Energy to the 21st Century: *Proceedings of the 15th Intersociety Energy Conversion Engineering Conference, Volume 1*, American Inst. of Aeronautics and Astronautics, Inc., c.1980, pp. 394-399.
19. Walker, Gilbert H.: Photovoltaic Conversion of Laser to Electrical Power. *18th Intersociety Energy Conversion Engineering Conference, Volume 3—Electrical Power Systems*, American Inst. of Chemical Engineers, c.1983, pp. 1194-1199.
20. Sze, S. M.: *Physics of Semiconductor Devices*, Second ed. John Wiley & Sons, Inc., c.1981.
21. Walker, G. H.; and Heinbockel, J. H.: Parametric Study of Laser Photovoltaic Energy Converters. *Sol. Cells*, vol. 22, no. 1, Sept. 1987, pp. 55-67.
22. Field, J. E., ed.: *The Properties of Diamond*. Academic Press Inc., 1979.
23. Bien, Darl D.; and Guentert, Donald C.: *A Method for Reducing the Equivalent Sink Temperature of a Vertically Oriented Radiator on the Lunar Surface*. NASA TM X-1729, 1969.
24. Advanced Space Programs, General Dynamics Space Systems Div.: *Orbital Transfer Vehicle Concept Definition and Systems Analysis Study—Final Report. Volume II—OTV Concept Definition and Evaluation, Book 4—Launch and Flight Operations*. NASA CR-179059, V.2, Bk. 4, 1986.
25. Davis, Eldon E.: *Future Orbital Transfer Vehicle Technology Study. Volume II Technical Report*. NASA CR-3536, 1982.
26. Sevastov, George E.; Schier, J. Alan; Iskenderian, Theodore C.; Lin, Yu-Hwan; Satter, Celeste M.; and Lehman, David H.: A Precision Pointing System for Space Telescope Class Optical Trackers. *A Collection of Technical Papers, Part 1—AIAA Guidance, Navigation and Control Conference*, Aug. 1988, pp. 452-470. (Available as AIAA-88-4107-CP.)
27. Yariv, Amnon: *Quantum Electronics*, Third ed. John Wiley & Sons, Inc., c.1989.
28. Waters, R. G.; Wagner, D. K.; Hill, D. S.; Tihanyi, P. L.; and Vollmer, B. J.: High-Power Conversion Efficiency Quantum Well Diode Lasers. *Appl. Phys. Lett.*, vol. 51, no. 17, Oct. 26, 1987, pp. 1318-1319.
29. Waters, R. G.; and Bertaska, R. K.: Degradation Phenomenology in (Al)GaAs Quantum Well Lasers. *Appl. Phys. Lett.*, vol. 52, no. 3, Jan. 18, 1988, pp. 179-181.
30. Munding, R.; Beach, R.; Bennett, W.; Solarz, R.; Krupke, W.; Staver, R.; and Tuckerman, D.: Demonstration of High-Performance Silicon Microchannel Heat Exchangers for Laser Diode Array Cooling. *Appl. Phys. Lett.*, vol. 53, no. 12, Sept. 19, 1988, pp. 1030-1032.

31. Garmire, Elsa M.; and Tavis, Michael T.: Heatsink Requirements for Coherent Operation of High-Power Semiconductor Laser Arrays. *IEEE J. Quantum Electron.*, vol. QE-20, no. 11, Nov. 1984, pp. 1277-1283.

32. Roychoudhuri, Chandrasekhar: Laser Beam Combining Technology. *Laser Diode Optics, Proceedings of SPIE The International Society for Optical Engineering*, Volume 740, David W. Kuntz, ed., 1987, pp. 66-69.

Table I. Optimized Converter Parameters

Width, $\mu\text{m}$	3.0
Thickness, $\mu\text{m}$	10.0
Donor concentration, $\text{cm}^{-3}$	$5 \times 10^{15}$
Acceptor concentration, $\text{cm}^{-3}$	$1 \times 10^{17}$
$p$ -surface recombination velocity, $\text{cm-sec}^{-1}$	$1 \times 10^3$
$n$ -surface recombination velocity, $\text{cm-sec}^{-1}$	$1 \times 10^3$
Width of $p$ -region, $\mu\text{m}$	2.5
Series resistance, $\Omega$	$1 \times 10^{-3}$
Input power density, $\text{W-cm}^{-2}$	$1 \times 10^3$
Number of junctions	500

Table II. Masses of Converter System Components for Lunar Habitat and Lunar Rover

Component	Mass, kg	
	Habitat	Rover
Converter	0.0111	0.0124
Diffuser	0.557	0.620
Diamond	0.362	0.821
Supporting blanket	2.7	0.675
Support structure	116	31.8
Beam-sized adjuster	6.67	6.97
Heat pipe radiator	9200	1330
Insulating blanket	Negligible	Negligible
Total converter system mass	$9.33 \times 10^3$	$1.37 \times 10^3$
Fuel and OTV mass	$38.7 \times 10^3$	$5.69 \times 10^3$
Mass of converter system, fuel, and OTV	$48.0 \times 10^3$	$7.06 \times 10^3$

Table III. Power System Components and Parameters

Component	Habitat	Rover
Solar collector/concentrator:		
Power collected, MW . . . . .	16.1	1.8
Concentration . . . . .	300	300
Aperture area, m <sup>2</sup> . . . . .	12 000	1322
Aperture diameter, m . . . . .	124	41.0
Solar constant, W/m <sup>2</sup> . . . . .	1365	1365
Focal length, m . . . . .	54	18
Aperture—axis intersection, m . . . . .	18	5.9
Surface area, m <sup>2</sup> . . . . .	12 994	1431
Mass (excluding radiators), kg . . . . .	1299	143
Surface reflection coefficient . . . . .	0.98	0.98
Solar photovoltaic array:		
Input power, MW . . . . .	8	0.9
Solar power conversion efficiency, percent . . . . .	22.5	22.5
Operating temperature, K . . . . .	353	353
Emission coefficient (front surface) . . . . .	0.5	0.5
Emission coefficient (rear surface) . . . . .	0.95	0.95
Area, m <sup>2</sup> . . . . .	40.0	4.4
Mass, kg . . . . .	98	11
Amplifier:		
Power input, MW . . . . .	3.6	0.4
Power output, MW . . . . .	2.5	0.28
No. of LDA's in output array . . . . .	500 626	55 148
No. of LDA's in amplifier . . . . .	505 683	55 705
LDA array output area, m <sup>2</sup> . . . . .	50	37
LDA array output diameter, m . . . . .	8	7
Mass, kg . . . . .	683	75
Laser diode array (LDA):		
Power output, W/LDA . . . . .	5	5
Wavelength, $\mu\text{m}$ . . . . .	0.85	0.85
Efficiency, percent . . . . .	70	70
Operating temperature, K . . . . .	300	300
Dimensions, cm . . . . .	1 × 1 × 0.6	2.7 × 2.7 × 0.6
Transmission optics:		
Mirror system mass, kg . . . . .	1020	756
Lens system mass, kg . . . . .	1255	927
Trusses:		
Length of main truss, m . . . . .	71.5	23.7
Mass of all trusses, kg . . . . .	1129	124

Table III. Concluded

Component	Habitat	Rover
<b>Radiators:</b>		
Temperature of main radiator, K . . . . .	353	353
Area of main radiator, m <sup>2</sup> . . . . .	3422	377
Diameter of main radiator, m . . . . .	66	22
Mass of main radiator, kg . . . . .	8898	980
Area of laser radiator, m <sup>2</sup> . . . . .	1648	182
Mass of laser radiator, kg . . . . .	4285	472
<b>Transmitter and receiver:</b>		
Orbital altitude, km . . . . .	2000	2000
Distance to horizon, km . . . . .	3310	3310
Beam area at horizon, m <sup>2</sup> . . . . .	0.6	0.8
Beam diameter at horizon, m . . . . .	0.86	1.0
Electrical output power at receiver, MW . . . . .	1.0	0.075
Photoconverter efficiency, percent . . . . .	47	32
Pointing accuracy, microradian . . . . .	1.0	1.0
Receiver dish diameter, m . . . . .	7.5	7.6
Beam coupling efficiency at receiver, percent . . . . .	85	85

Table IV. Power System Mass Summary and Totals for Lunar Habitat and Lunar Rover

Component	Mass, kg	
	Habitat	Rover
Amplifier	683	75
Solar photovoltaic array	98	11
Collector/concentrator	1 299	143
Main radiator	8 898	980
Laser radiator	4 285	472
Trusses	1 129	124
Transmission optics	2 275	1 683
Satellite	18 667	3 488
Fuel and OTV	36 446	7 740
Satellite, fuel, and OTV	55 113	11 228

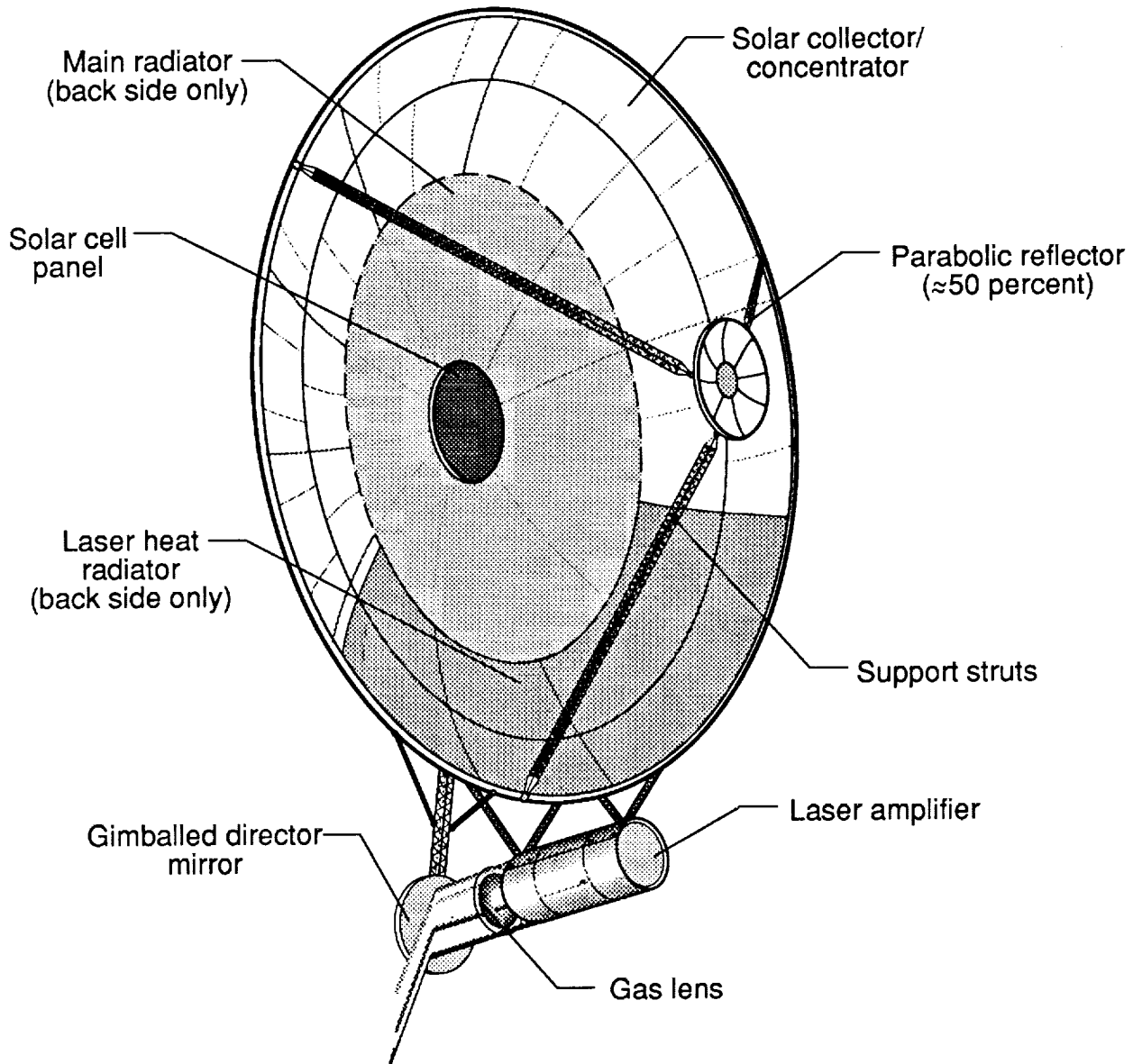


Figure 1. Diode laser satellite.

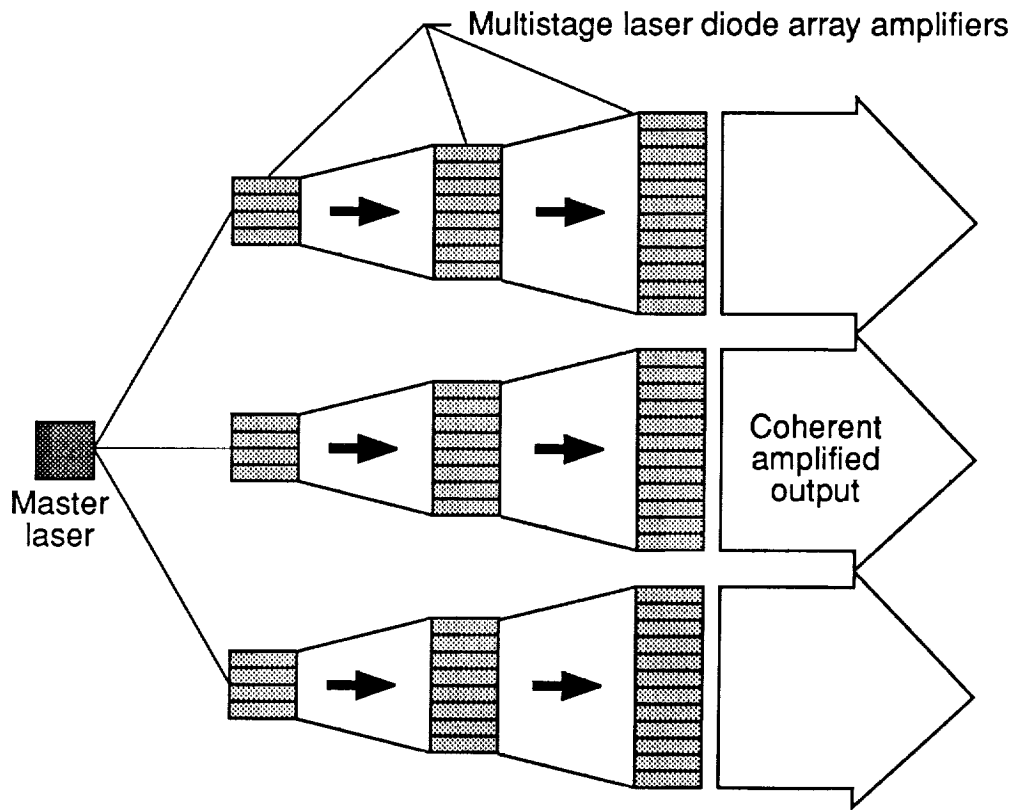


Figure 2. Multistage, large-scale array amplifier.

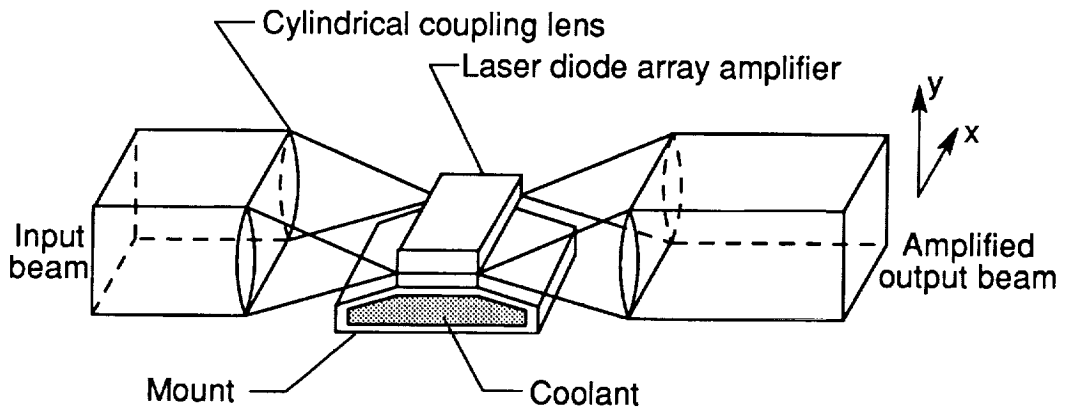


Figure 3. Laser diode array amplifier element.

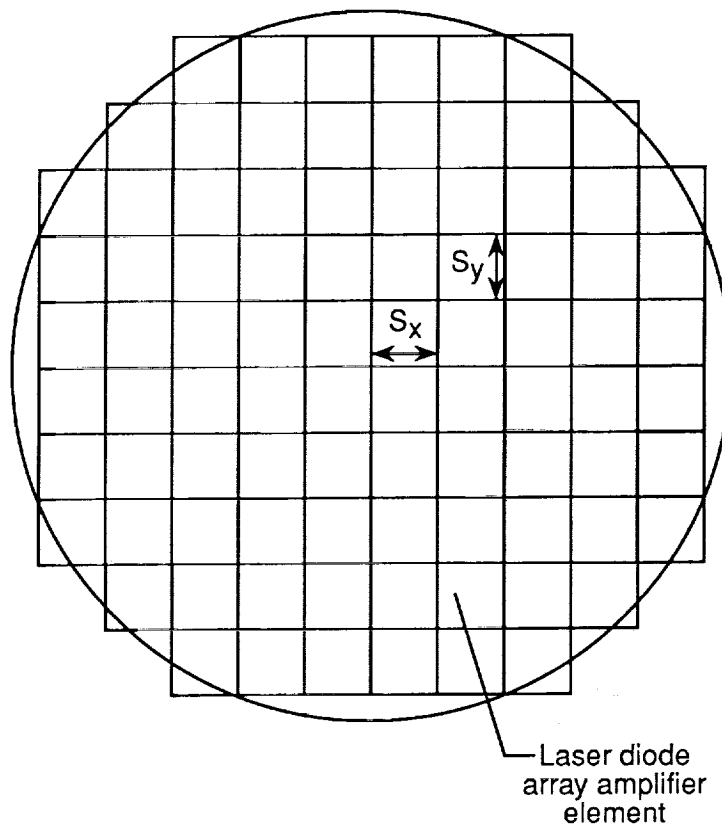


Figure 4. Output aperture of large-scale array. Not to scale.

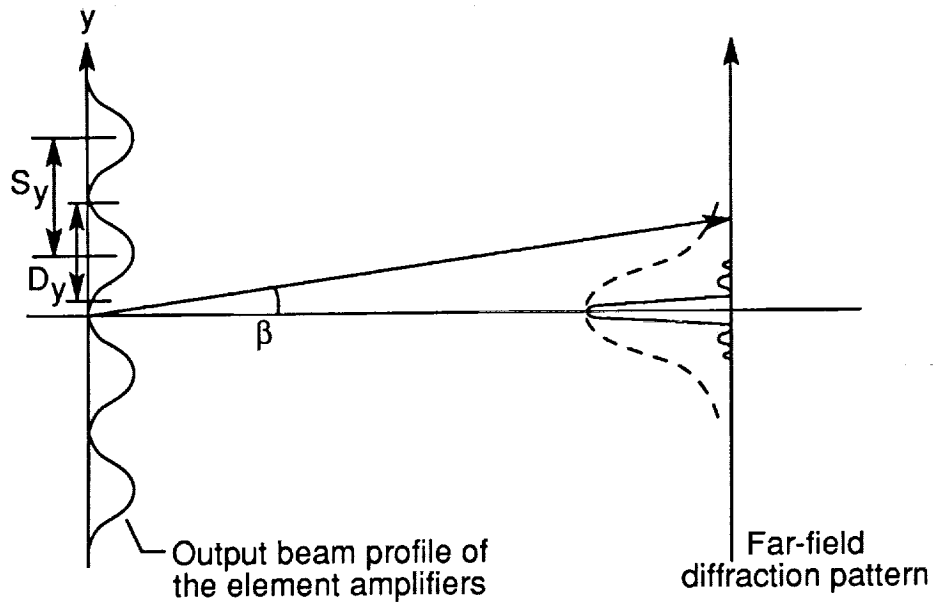


Figure 5. One-dimensional far-field diffraction pattern of output array;  $D_y$  is the beam width and  $S_y$  is the separation between amplifier elements;  $\alpha$  (not shown) is an angle perpendicular to plane of  $\beta$ .

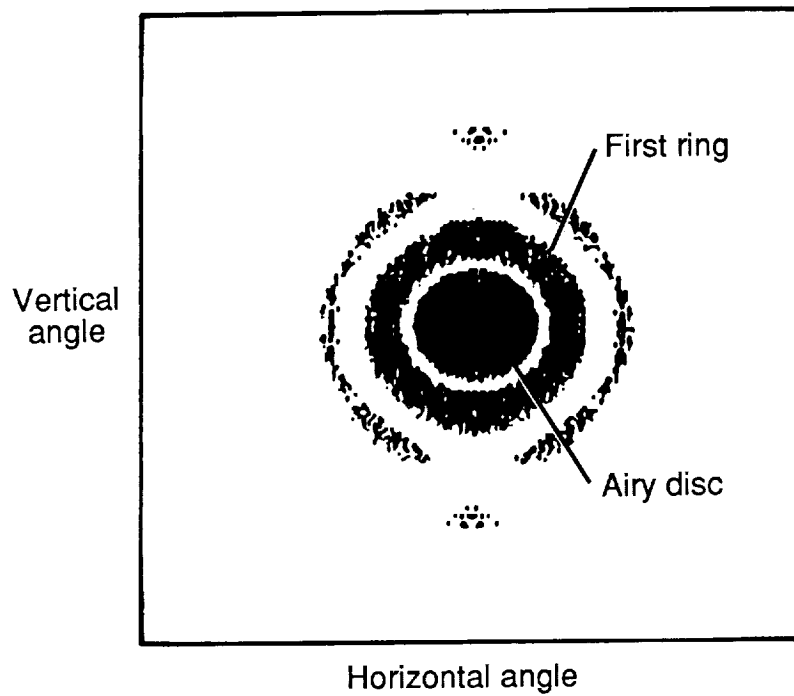


Figure 6. Detailed structure of the central far-field pattern.

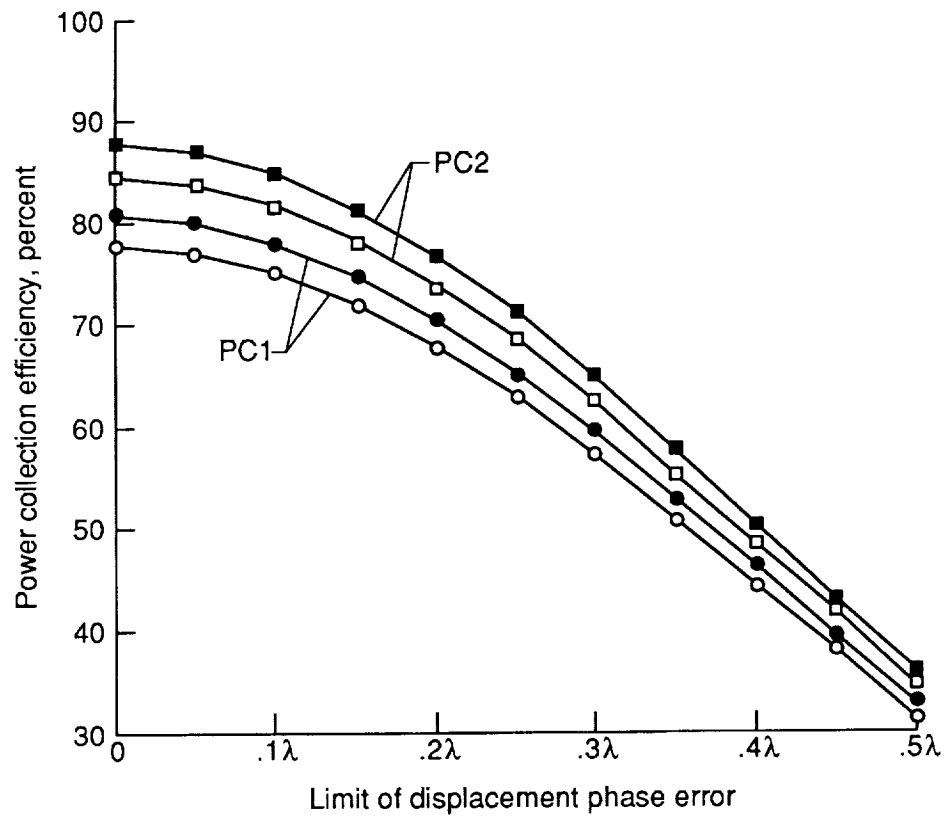


Figure 7. Power collection efficiency versus displacement phase error.

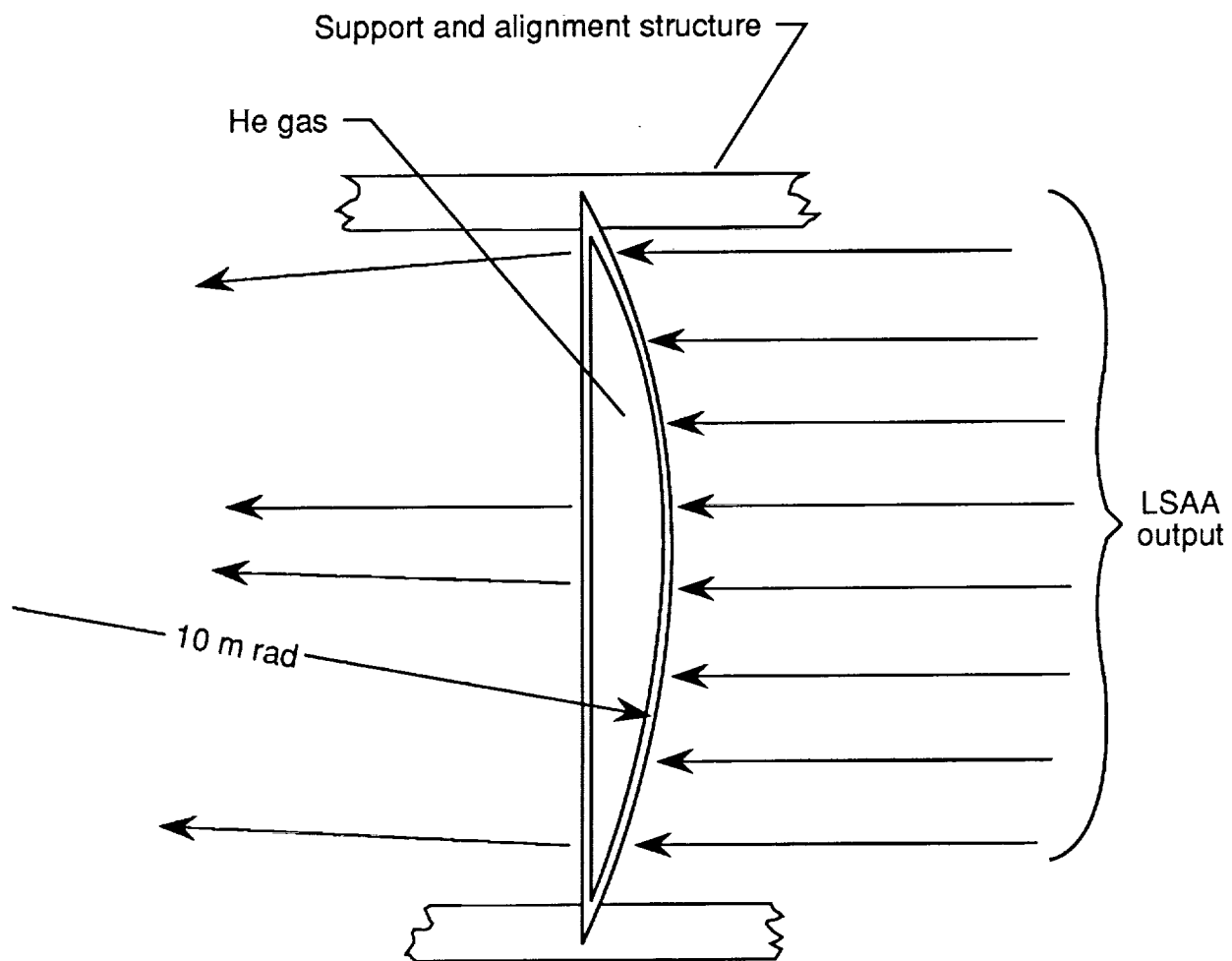


Figure 8. Gas lens. Not to scale.

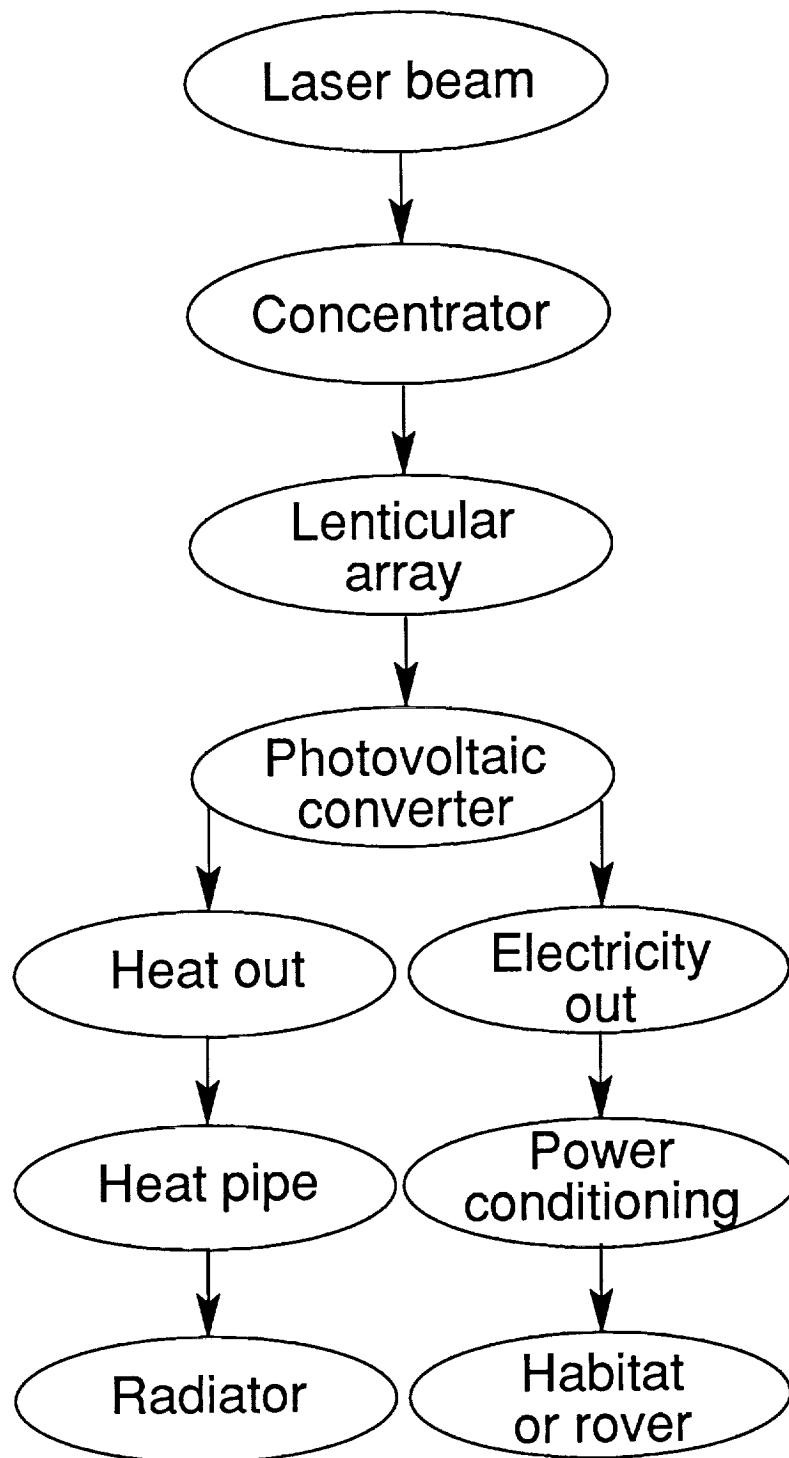


Figure 9. Flow diagram for converter assembly.

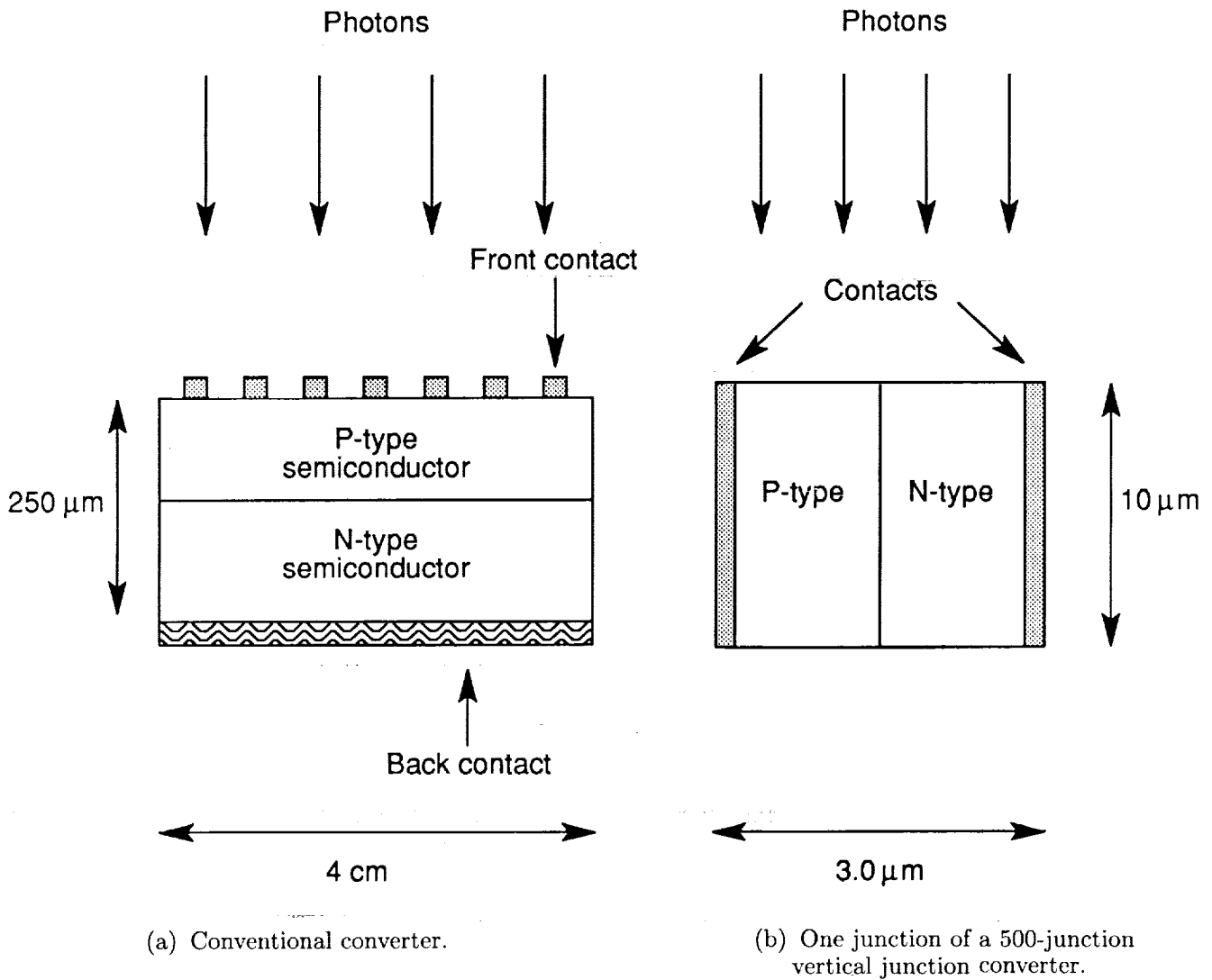


Figure 10. Photovoltaic converters.

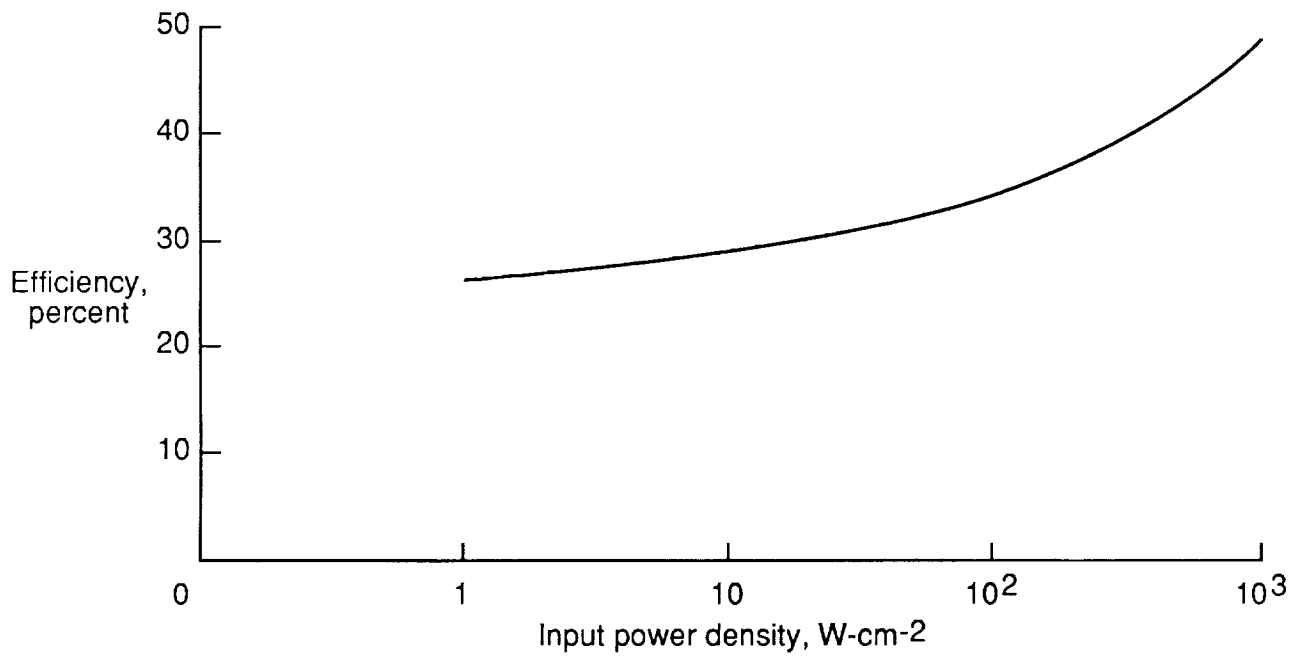


Figure 11. Converter efficiency versus input power density. Optimized 0.85  $\mu\text{m}$  converter (1.46 eV), 500 junctions.

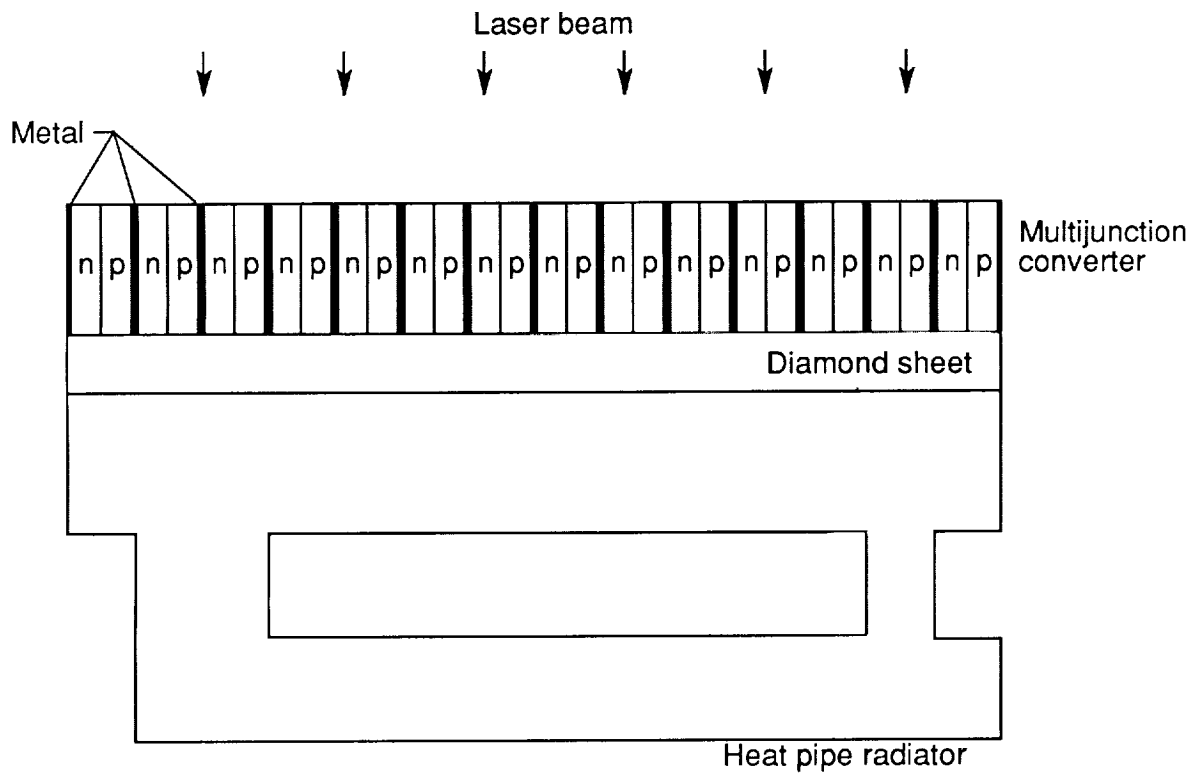


Figure 12. Schematic diagram of converter radiator system.

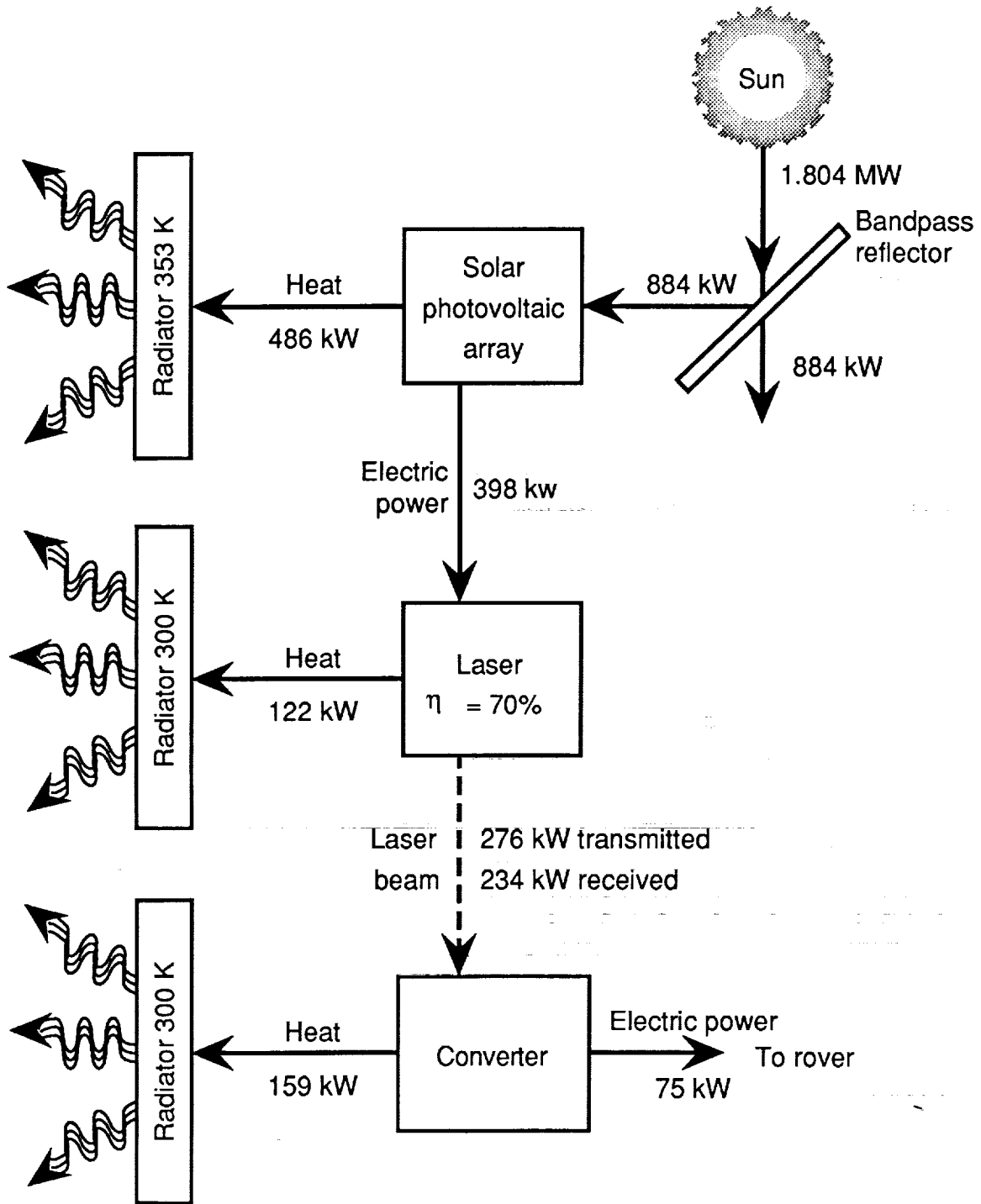


Figure 13. Power flow of laser satellite for rover.

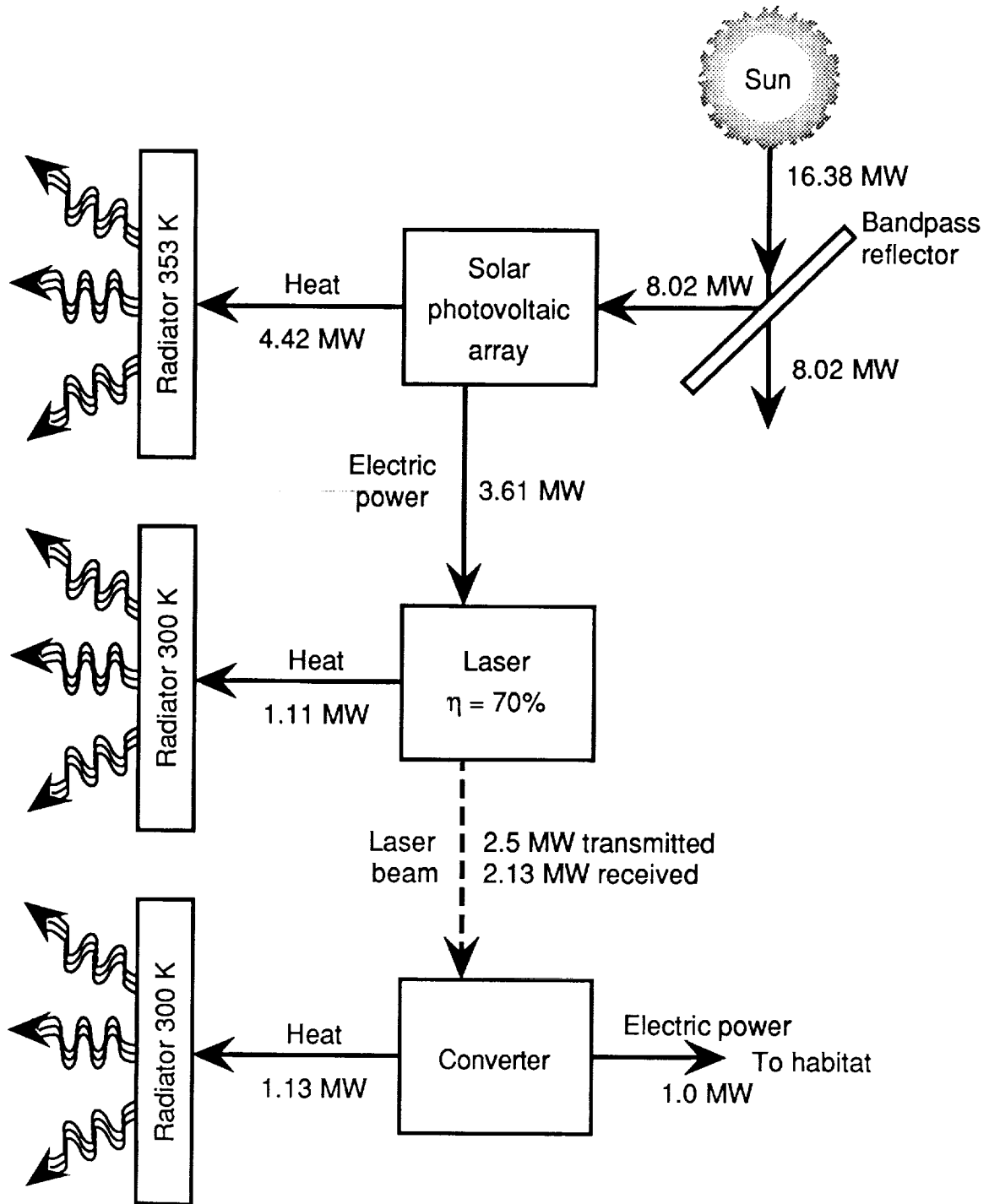


Figure 14. Power flow of laser satellite for habitat.

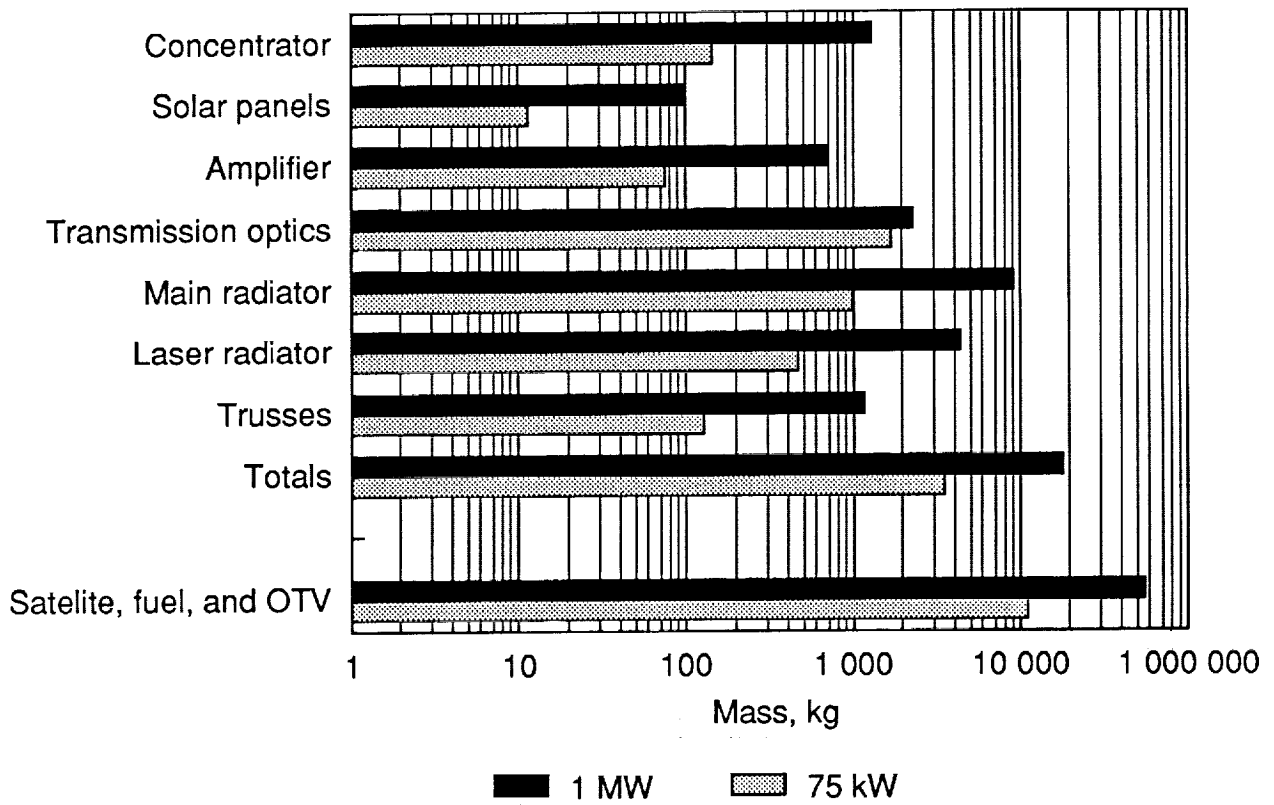
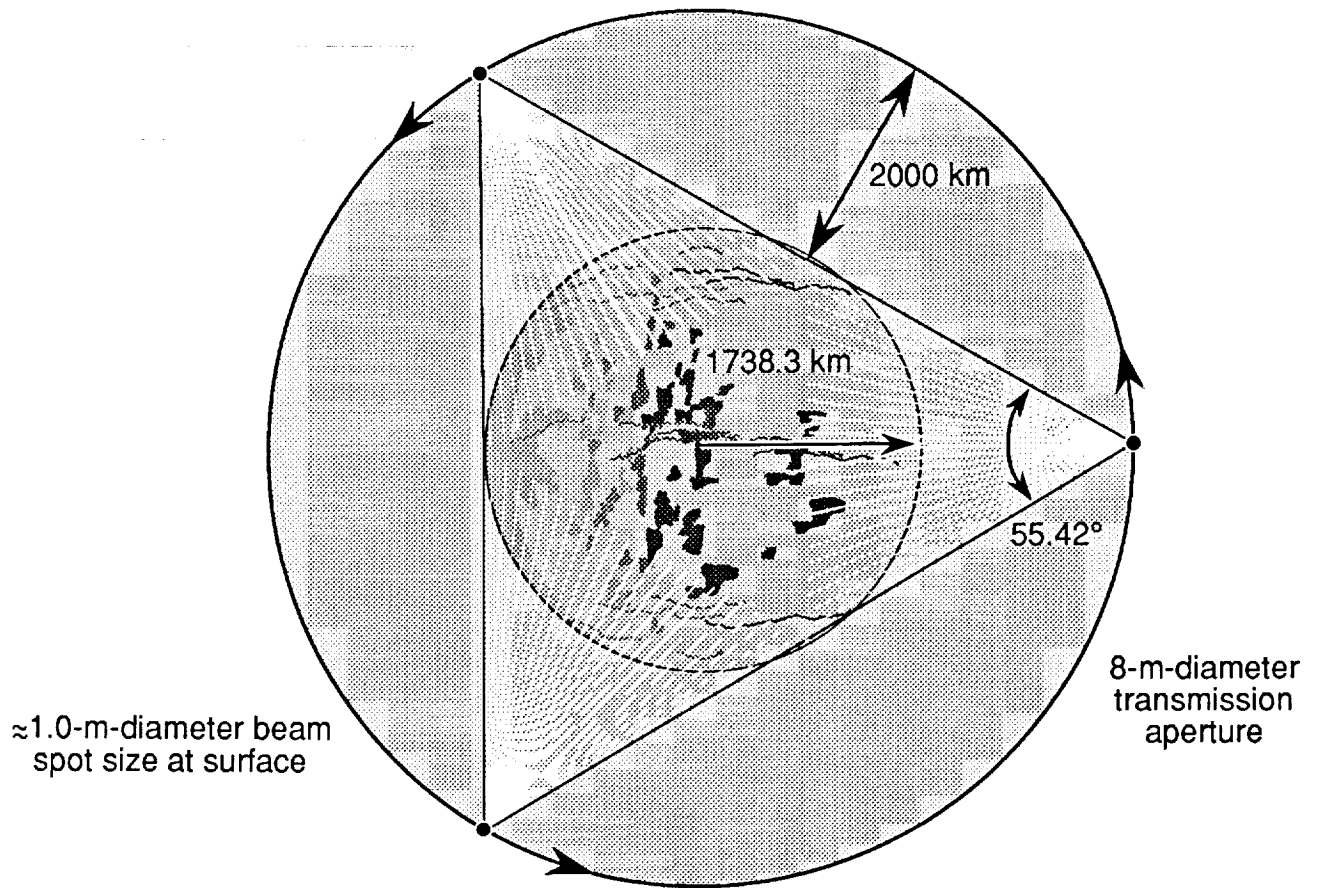


Figure 15. Satellite component masses.



Orbital velocity.....	1146 m/sec
Orbital period.....	5.7 hr
Time in view.....	1.97 hr
Time two satellites in view.....	4 min 21 sec (in orbital plane)

Figure 16. Lunar orbit data.

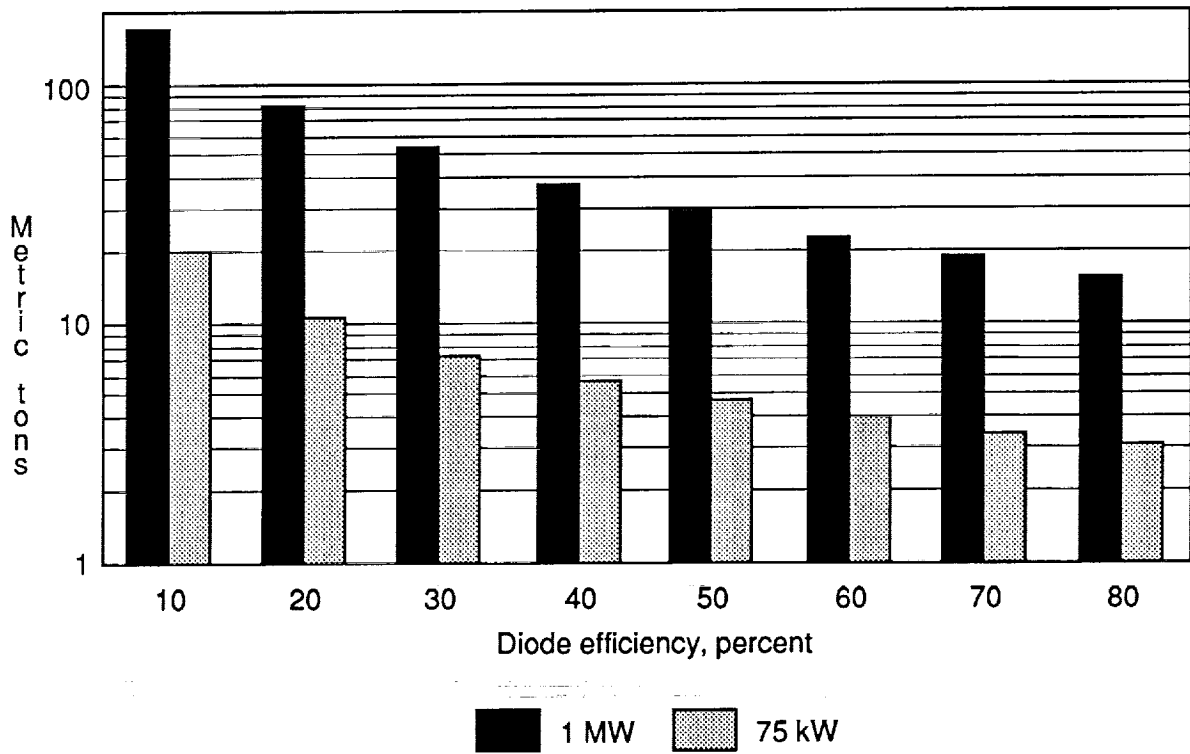


Figure 17. Satellite mass variation versus laser diode efficiency. (Coupling efficiency = 85 percent.)

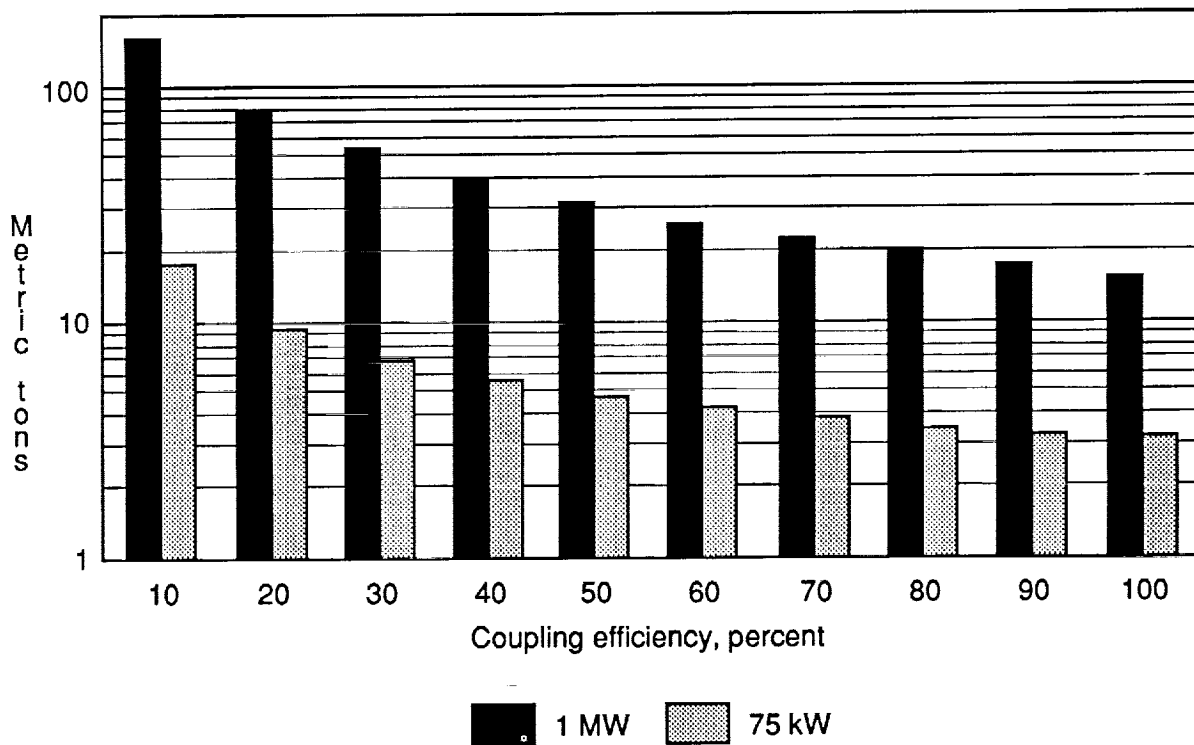


Figure 18. Satellite mass variation versus coupling efficiency. (Diode efficiency = 70 percent.)



Report Documentation Page

1. Report No. NASA TP-2992		2. Government Accession No.		3. Recipient's Catalog No.	
4. Title and Subtitle Diode Laser Satellite Systems for Beamed Power Transmission				5. Report Date July 1990	
				6. Performing Organization Code	
7. Author(s) M. D. Williams, J. H. Kwon, G. H. Walker, and D. H. Humes				8. Performing Organization Report No. L-16669	
9. Performing Organization Name and Address NASA Langley Research Center Hampton, VA 23665-5225				10. Work Unit No. 506-41-41-01	
				11. Contract or Grant No.	
12. Sponsoring Agency Name and Address National Aeronautics and Space Administration Washington, DC 20546-0001				13. Type of Report and Period Covered Technical Paper	
				14. Sponsoring Agency Code	
15. Supplementary Notes M. D. Williams, G. H. Walker, and D. H. Humes: Langley Research Center, Hampton, Virginia. J. H. Kwon: Miami University, Oxford, Ohio.					
16. Abstract This paper describes a power system composed of an orbiting laser satellite and a surface-based receiver/converter. Power is transmitted from the satellite to the receiver/converter by laser beam. The satellite components are (1) solar collector, (2) photovoltaic cells, (3) heat radiators, (4) laser system, and (5) transmission optics. The receiver/converter components are (1) receiver dish, (2) lenticular lens, (3) photocells, and (4) heat radiator. Although the system can be adapted to missions at many locations in the solar system, only two are examined here: (1) powering a lunar habitat and (2) powering a lunar rover. Power system components are described and their masses, dimensions, operating powers, temperatures, etc., are estimated using known or feasible component capabilities. The critical technologies involved are discussed and other potential missions are mentioned.					
17. Key Words (Suggested by Authors(s)) Diode lasers Power transmission Satellite Lunar missions			18. Distribution Statement Unclassified—Unlimited  Subject Category 36		
19. Security Classif. (of this report) Unclassified		20. Security Classif. (of this page) Unclassified		21. No. of Pages 29	22. Price A03

